AD-A133 853 RESEARCH ON AERO-THERMODYNAMIC DISTORTION INDUCED 1/2
STRUCTURAL DYNAMIC RESP.. (U) PURDUE UNIV LAFAYETTE IN
SCHOOL OF MECHANICAL ENGINEERING S FLEETER JUN 83
UNCLASSIFIED ME-TSPC-TR-83-04 AFOSR-TR-83-0737 F/G 21/5 NL

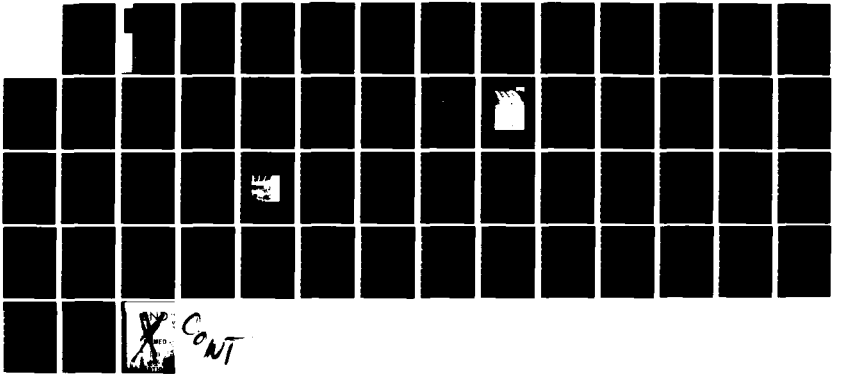

CONT

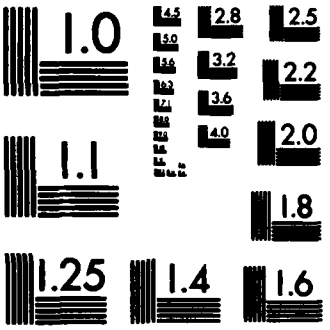

MICROCOPY RESOLUTION TEST CHART
NATIONAL BUREAU OF STANDARDS-1963-A

AFOSR-TR- 83-0737

Report ME-TSPC-TR-83-04

June 1983

Annual Summary Report

Grant AF 820188

Research on Aero-Thermodynamic Distortion Induced Structural Dynamic Response of Multi-Stage Compressor Blading

Sanford Fleeter

Thermal Science and Propulsion Center

School of Mechanical Engineering

Purdue University

West Lafayette, Indiana 47907

Prepared for

Directorate of Aerospace Sciences

Air Force Office of Scientific Research

UNCLASSIFIED

SECURITY CLASSIFICATION OF THIS PAGE (When Data Entered)

REPORT DOCUMENTATION PAGE	READ INSTRUCTIONS BEFORE COMPLETING FORM
1. REPORT NUMBER: AFOSR-TR- 83-0737	2. GOVT ACCESSION NO.: AD-A133 853
	3. RECIPIENT'S CATALOG NUMBER
4. TITLE (and Subtitle): RESEARCH ON AERO-THERMODYNAMIC DISTORTION INDUCED STRUCTURAL DYNAMIC RESPONSE OF MULTI-STAGE COMPRESSOR BLADING	5. TYPE OF REPORT & PERIOD COVERED: ANNUAL 15 Apr 82 - 14 Apr 83
	6. PERFORMING ORG. REPORT NUMBER
7. AUTHOR(s): SANFORD FLEETER	8. CONTRACT OR GRANT NUMBER(s): AFOSR-82-0188
9. PERFORMING ORGANIZATION NAME AND ADDRESS: PURDUE UNIVERSITY, DEPT OF MECHANICAL ENGINEERING, WEST LAFAYETTE, IN 47907	10. PROGRAM ELEMENT, PROJECT, TASK AREA & WORK UNIT NUMBERS: 61102F, 2307/A4
11. CONTROLLING OFFICE NAME AND ADDRESS: AIR FORCE OFFICE OF SCIENTIFIC RESEARCH/NA, BOLLING AFB, DC 20332	12. REPORT DATE: June 1983
	13. NUMBER OF PAGES: 49
14. MONITORING AGENCY NAME & ADDRESS(if different from Controlling Office)	15. SECURITY CLASS. (of this report): Unclassified
	15a. DECLASSIFICATION DOWNGRADING SCHEDULE

16. DISTRIBUTION STATEMENT (of this Report)

Approved for Public Release; Distribution Unlimited.

17. DISTRIBUTION STATEMENT (of the abstract entered in Block 20, if different from Report)

18. SUPPLEMENTARY NOTES

19. KEY WORDS (Continue on reverse side if necessary and identify by block number)

TURBOMACHINERY
COMPRESSORS
FORCED VIBRATION
FLUID MECHANICS
AERO-THERMODYNAMIC DISTORTION
UNSTEADY FLOW
INLET FLOW

20. ABSTRACT (Continue on reverse side if necessary and identify by block number)

The structural dyanmic response of turbomachinery components to aero-thermodynamic distortion induced excitations is an item of major concern in the design of advanced gas turbine engines. The rotor speeds at which these resonant forced responses occur can be predicted with Campbell diagrams. However, due to the inadequacies of the existing time-variant aerodynamic models, no accurate prediction can currently be made for the amplitude of the resulting stresses. The overall objective of this research program is to quantitatively investigate the fundamental phenomena relevant to

DD FORM 1 JAN 73 1473 EDITION OF 1 NOV 65 IS OBSOLETE

UNCLASSIFIED

SECURITY CLASSIFICATION OF THIS PAGE (When Data Entered)

aerothermodynamic distortion induced structural dynamic blade response in multi-stage gas turbine fans and compressors. Unique unsteady aerodynamic data will be obtained to validate and indicate necessary refinements to state-of-the-art analyses and to direct the modeling of new analyses. Also, for the first time, a first principles capability to predict the vibrational response amplitude of blading due to aerodynamic excitations will be developed. This report summarizes the progress and results obtained during the first year of this program. These include: the dynamic instrumentation of the first-state vane row of a three-stage research compressor; the design, specification and initiation of the development of the dynamic data acquisition and analysis system; the initiation of the development of the necessary data analysis and calibration techniques; and the theoretical development of a unique coupled mode structural dynamic blade response analysis based on an energy balance technique.

Report ME-TSPC-TR-83-04

ANNUAL SUMMARY REPORT

GRANT AF 820188

RESEARCH ON AERO-THERMODYNAMIC DISTORTION INDUCED STRUCTURAL DYNAMIC RESPONSE OF MULTI-STAGE COMPRESSOR BLADING

SANFORD FLEETER

June 1983

Thermal Sciences and Propulsion Center
School of Mechanical Engineering
Purdue University
West Lafayette, Indiana 47907

Prepared for

Directorate of Aerospace Sciences
Air Force Office of Scientific Research

ABSTRACT

The structural dynamic response of turbomachinery components to aero-thermodynamic distortion-induced excitations is an item of major concern in the design of advanced gas turbine engines. The rotor speeds at which these resonant forced responses occur can be predicted with Campbell diagrams. However, due to the inadequacies of the existing time-variant aerodynamic models, no accurate prediction can currently be made for the amplitude of the resulting stresses.

The overall objective of this research program is to quantitatively investigate the fundamental phenomena relevant to aero-thermodynamic distortion-induced structural dynamic blade response in multi-stage gas turbine fans and compressors. Unique unsteady aerodynamic data will be obtained to validate and indicate necessary refinements to state-of-the-art analyses and to direct the modeling of new analyses. Also, for the first time, a first principles capability to predict the vibrational response amplitude of blading due to aerodynamic excitations will be developed.

This report summarizes the progress and results obtained during the first year of this program. These include: the dynamic instrumentation of the first-stage vane row of a three-

stage research compressor; the design, specification, and initiation of the development of the dynamic data acquisition and analysis system; the initiation of the development of the necessary data analysis and calibration techniques; and the theoretical development of a unique coupled mode structural dynamic blade response analysis based on an energy balance technique.

TABLE OF CONTENTS

1. INTRODUCTION

The structural dynamic response of fan, compressor, and turbine blading to aero-thermodynamic distortion induced excitations is an item of rapidly increasing concern to designers and manufacturers of gas turbine engines for advanced technology applications. Destructive aerodynamic forced responses of gas turbine engine blading have been generated by a wide variety of aero-thermodynamic distortion sources. These include: blade wakes; multi-staging interaction effects; large angle of attack or yaw; engine exhaust recirculation; cross-flow at the inlet; pressure variations on the engine due to external aerodynamics; and armament firing. The following physical phenomena have been identified as being significant with regard to aero-thermodynamic distortion induced structural dynamic responses of fan and compressor blading.

* Resonance
* Multi-stage interactions
* Stall
* Inlet gusts
* Time-varying inlet flows

* Flow separation

* Potential effects

* Turbulence

The first principles prediction of the structural dynamic response associated with all of the above physical phenomena is identical and involves the following elements. Spatially periodic variations in pressure, velocity, temperature, and flow direction of the exit flow field of an upstream element appear as temporally varying in a coordinate system fixed to the downstream row. As a result, individual airfoils are subject to a time-variant aerodynamic forcing function which can induce high level vibratory stresses.

The analysis of the aerodynamically forced response vibratory behavior of a blade or vane row requires a definition of the unsteady forcing function in terms of its harmonics. The time-variant aerodynamic response of the airfoil to each harmonic of this forcing function is then assumed to be comprised of two parts. One is due to the disturbance being swept past the non-responding fixed airfoils. The second arises when the airfoils respond to this disturbance. Mathematically these effects are modeled by two distinct analyses. A linearized small perturbation gust analysis is used to predict the time-variant aerodynamics of the fixed non-responding airfoils to each harmonic of the disturbance. A self-induced unsteady aerodynamic analysis

wherein the airfoils are assumed to be harmonically oscillating is then used to predict the additional aerodynamic effects due to the airfoil response. Superposition of these two effects can be performed only with knowledge of the modal pattern and amplitude of response of the blading because the magnitude of the pressure field resulting from the airfoil motion is dependent upon the amplitude of this motion. Thus a solution with key elements consisting of the gust analysis, a self-induced unsteady aerodynamic analysis, and an airfoil structural analysis is necessary to predict the total response of an airfoil subjected to an upstream generated spatially periodic disturbance.

The unsteady small perturbation gust and self-induced unsteady aerodynamic analyses are two-dimensional and, as such, are coupled to the airfoil structural analysis by means of a strip theory approximation. Thus, the airfoil is considered to consist of a series of individual and independent two-dimensional aerodynamic regions. The time-variant aerodynamic analyses are then applied to each such individual region, with the characteristic parameters including the Mach number, reduced frequency, stagger angle, and solidity, taken as the average value at the inlet boundary. It should be noted that there is no coupling between adjacent aerodynamic regions. Hence, aerodynamic forced vibrations involving spanwise variations in unsteady aerodynamics cannot be treated, i.e., if spanwise variatins exist in the aerodynamic forcing f'nction ot caused by simple inlet spanwise variatins in the Mach .umber, reduced frequency, stagger angle,

or solidity, such a strip theory design system is of no value. Some of the previously noted forced response sources may fit into this category, as for example, the case of rotor tip vortices generating a forced response in a downstream blade or vane row.

II. PROGRAM OBJECTIVES

Overall Objectives

The overall objective of this research program is to quantitatively investigate the fundamental phenomena relevant to distortion generated aero-thermodynamic induced structural dynamic effects in gas turbine engine blade rows. Unique unsteady aerodynamic data will be obtained on stationary and rotating blade rows to validate and indicate necessary refinements to current state-of-the-art analyses and to direct the modeling and development of new analyses. Also, for the first time, a first principles capability to predict the vibrational response amplitude of blading due to aerodynamic excitations based on an energy balance technique will be developed.

From first principles considerations, the relevant fundamental physical phenomena are identical for the various sources of aero-thermodynamic distortion. Hence, to accomplish this overall objective in a timely and efficient manner, while obtaining results of direct interest and significance to the gas turbine engine community, this proposed research program is concerned with the time-variant aerodynamics and structural dynamic response of multi-stage stationary and rotating blade rows, with the primary source of excitation initially being the wakes from upstream blade elements. The overall objective includes the following.

* The experimental determination of the fundamental time-variant gust aerodynamics associated with variations in incidence angle (loading), reduced frequency, solidity, and multi-stage effects on both stationary and rotating blade rows as well as the investigation of the validity of:
  * the two-dimensional linearity and superpositioning assumptions;
  * the small perturbation modeling concept;
* The development of a first principles state-of-the-art capability to predict the vibrational response amplitude of blading based on an energy balance technique, with key elements consisting of the following coupled existing analyses:
  * a flat plate cascade transverse gust analysis;
  * a flat plate cascade self-induced unsteady aerodynamics analysis;
  * an airfoil structural analysis.

Thus, this program is directed at providing fundamental time-variant aerodynamic data which will not only validate and indicate refinements to the current state-of-the-art two-dimensional gust analyses but will also address the validity of the most basic assumptions inherent in these analyses and in the structure of forced response design systems. In addition a state-of-the-art first prinicples predictive aerodynamically forced response analysis based on an energy balance technique will be developed.

Specific Objectives

The following were the specific objectives for the first year of this research program.

* Dynamic instrumentation of the first stage vane row of the three-stage research compressor;

* Design, specification, and initiation of the development of the dynamic data acquisition system;

* Initiation of the development of the necessary data analysis and calibration techniques;

* Theoretical development of a coupled mode structural dynamic blade response analysis based on an energy balance technique.

III. TECHNICAL APPROACH

The technical approach to achieve the overall program objectives requires that extensive, high-quality, detailed aerodynamic data be acquired from benchmark experiments which model the fundamental flow physics of aero-thermodynamic induced structural dynamic effects in gas turbine engines. These data must be analyzed and correlated with appropriate state-of-the-art analyses to ascertain their range of validity and/or to indicate necessary refinements. In addition, advanced mathematical models and techniques for the prediction of these phenomena will be developed and experimentally verified.

The approach to achieving these experimental objectives is to measure the time-variant pressure distribution in controlled benchmark experiments which model the fundamental flow physics and thereby identify and quantify the key unsteady aerodynamic parameters relevant to aero-thermodynamic distortion induced response of blading. In particular, this research program is aimed at measuring the fundamental unsteady gust aerodynamics associated with variations in incidence angle (loading), reduced frequency, solidity, multi-stage effects, as well as investigating the validity of the two-dimensional linearity and superpositioning assumptions and the applicability of the small perturbation modeling concept. This requires obtaining airfoil surface chordwise and spanwise unsteady pressure data on both stationary

and rotating blade rows as well as detailed inlet and exit plane flow surveys in a multi-stage axial flow compressor. These data will be correlated with state-of-the-art unsteady cascade transverse gust analyses and will be used to determine their range of validity and to direct the development of an advanced first principles forced vibration aerodynamic analysis which the designer can use with confidence. In addition, a unique first principles predictive aerodynamically forced response analysis will be developed based on an energy balance technique.

Facility

In the first stage of a multi-stage axial flow compressor the wakes from the upstream rotor blades are the source of the aerodynamically induced fluctuating surface pressures on the downstream stator vanes, i.e., the rotor blade wakes define the forcing function to the downstream stator vane row. In the aft stages of the compressor the wakes from all of the upstream blading, both rotors and stators, are the source of the aerodynamically induced fluctuating surface pressure distributions on the downstream stator vane and rotor blade rows. Hence, it is necessary to experimentally model all of the significant features which define this forcing function. These include the variation of incidence, the wave form, the velocity (pressure) variation, the various blade row interactions in a multi-stage machine, and the reduced frequency ($k = \omega C / 2V_{axial}$) which defines the order of magnitude of the unsteadiness. (Forced response problems in

turbomachines typically have first harmonic reduced frequency values varying from 0.2 to 8.0.) The above noted features can all be simulated in the Purdue University Multi-Stage Axial Flow Research Compressor.

Figure 1 presents a schematic of the overall facility, with the compressor test section shown in greater detail in Figures 2 and 3. The three identical rotor-stator stages are in an annulus with constant hub (0.300 m) and tip (0.420 m) diameters. All of the vane rows have 41 identical stators which are mounted on separate interchangeable ring assemblies which can be independently moved. The overall airfoil and compressor characteristics are presented in Table 1.

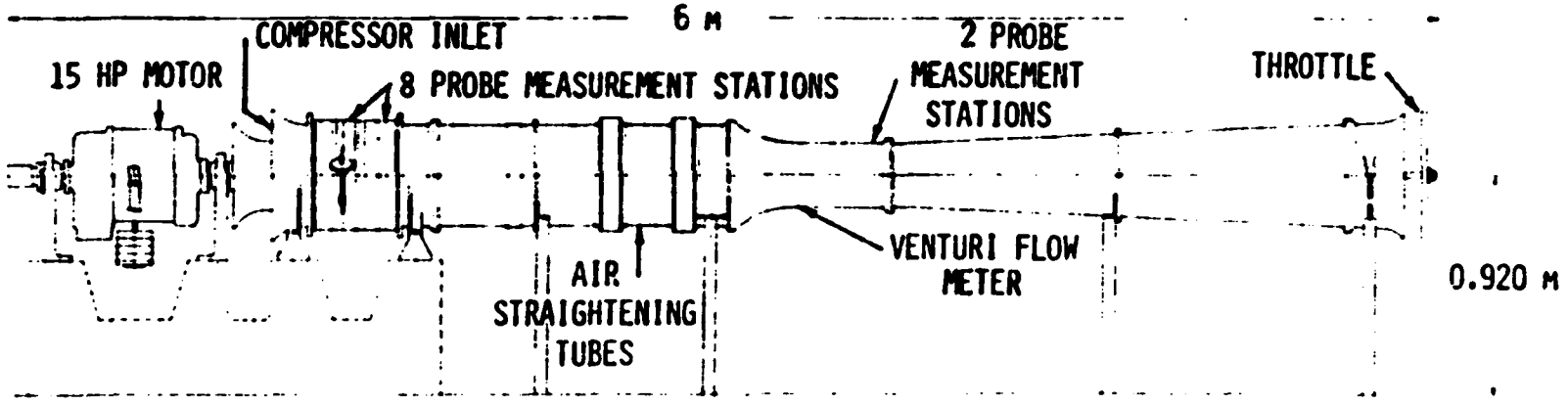

Figure 1. Schematic of overall facility.

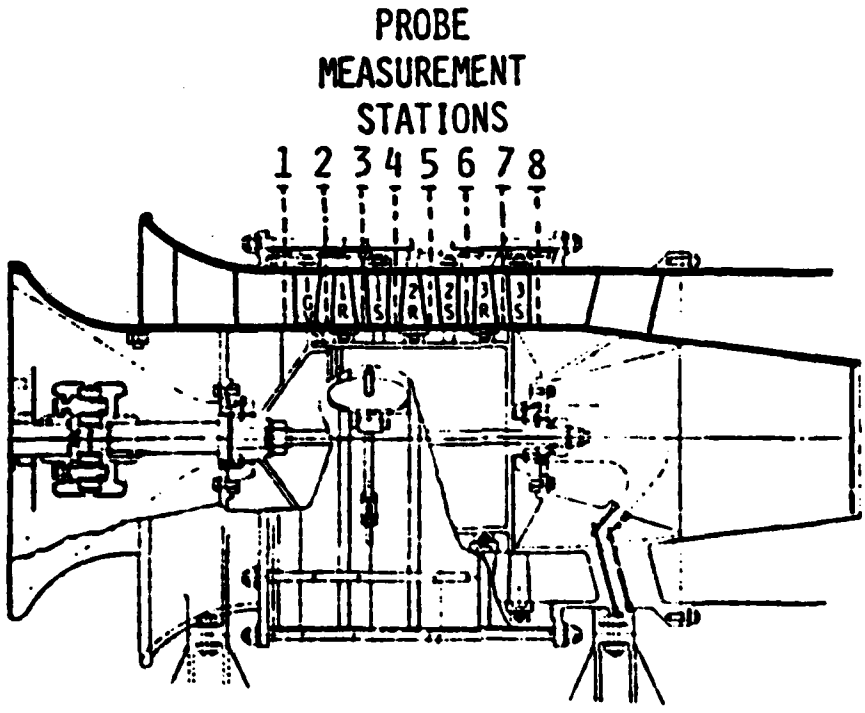

Figure 2. Schematic of compressor test section.

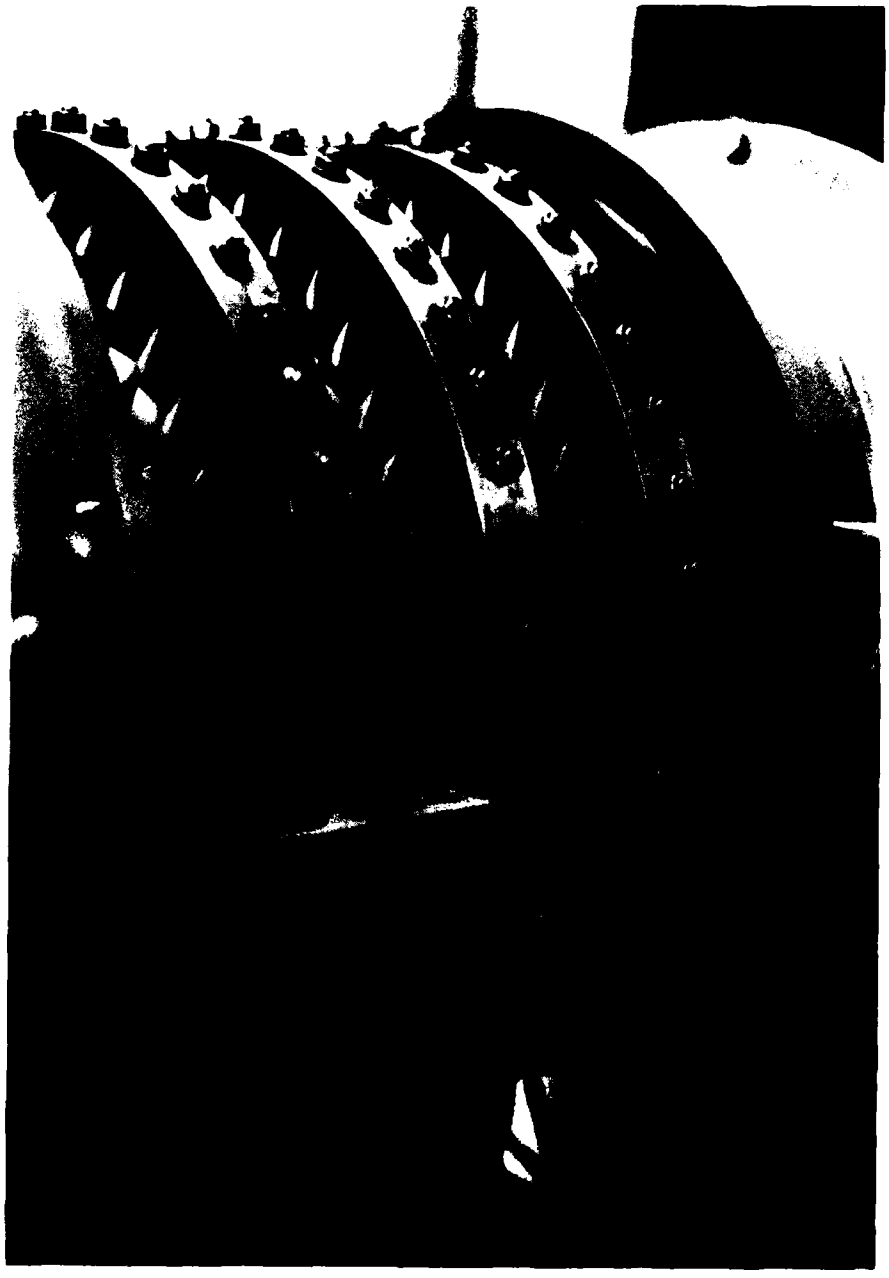

Figure 3. Close-Up View of the Blading of the Three-Stage Research Compressor.

TABLE I

AIRFOIL MEAN SECTION CHARACTERISTICS AND

COMPRESSOR DESIGN POINT CONDITIONS

	Rotor	Stator
Type of Airfoil	C4	C4
Number	43	41
Chord, C(mm)	30	30
Solidity, C/S	1.09	1.14
Aspect Ratio	2.0	2.0
Thickness/Chord (%)	10	10
Flow Rate (kg/second)	2.66	
Design Axial Velocity (meters/sec)	32.0	
Rotational Speed (RPM)	3000	
Number of States	3	
Stage Pressure Ratio	1.003	
Inlet Tip Diameter (mm)	420	
Hub/Tip Radius Ratio	0.715	
Stage Efficiency, (%)	85	

IV. PROGRAM STATUS AND RESULTS

All of the previously noted specific objectives established for the first year of this research program have been successfully met.

* Dynamic Instrumentation of First Stage Vanes

The dynamic instrumentation for this series of experiments has been specified and designed. For instrumentation purposes, a number of stator vanes have been fabricated from cast aluminum. In conjunction with Kulite Corporation, these aluminum airfoils have been instrumented along the hub, mean, and tip streamlines with Kulite thin-line design dynamic pressure transducers.

A structural vibrations analysis has been performed on the stator vanes. Figure 4 depicts the finite element representation of the stator. The first and second bend and first torsion mode shapes and frequencies are presented in Figures 5 through 7. Based on these results, a Campbell diagram for the first stage vane row was constructed, Figure 8. The 43 E line represents the first stage rotor blade excitation source.

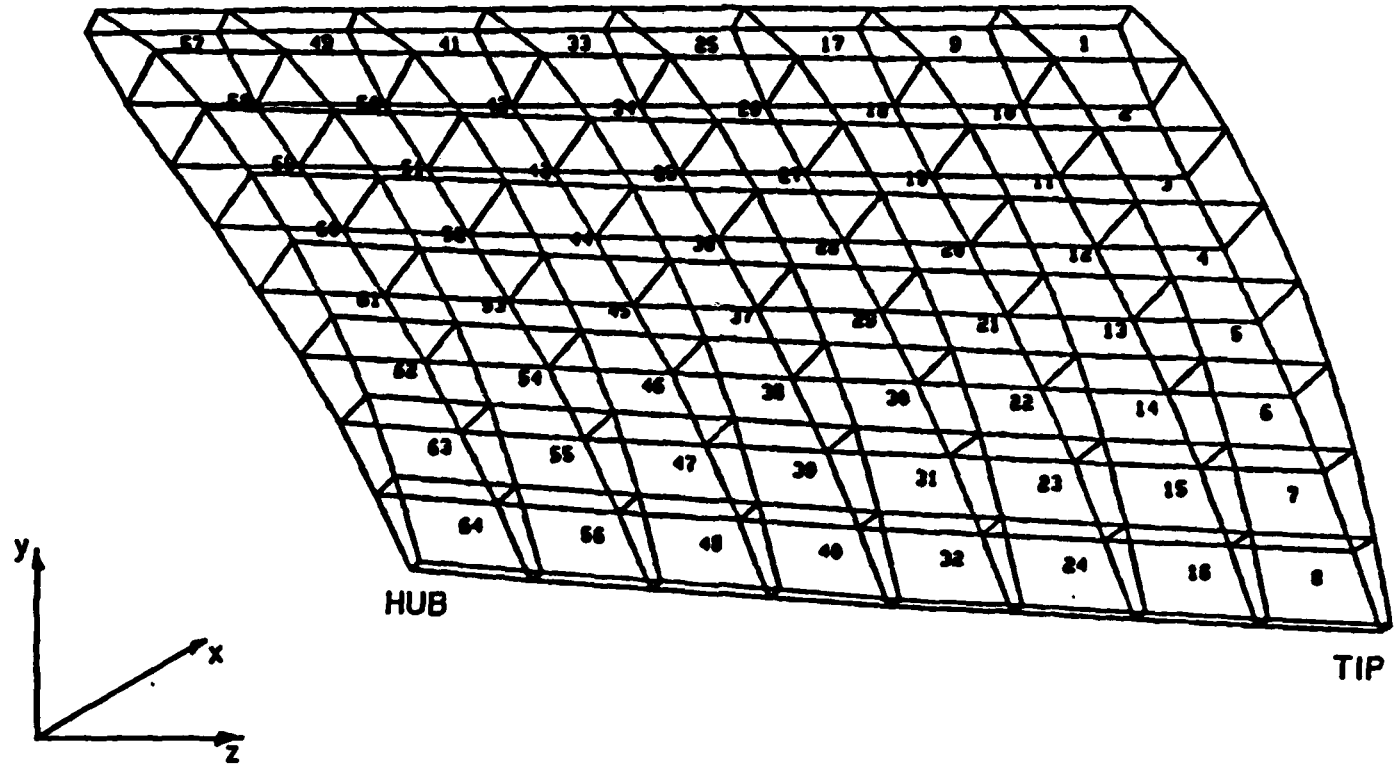

Figure 4. Finite Element Representation of Stator Vane.

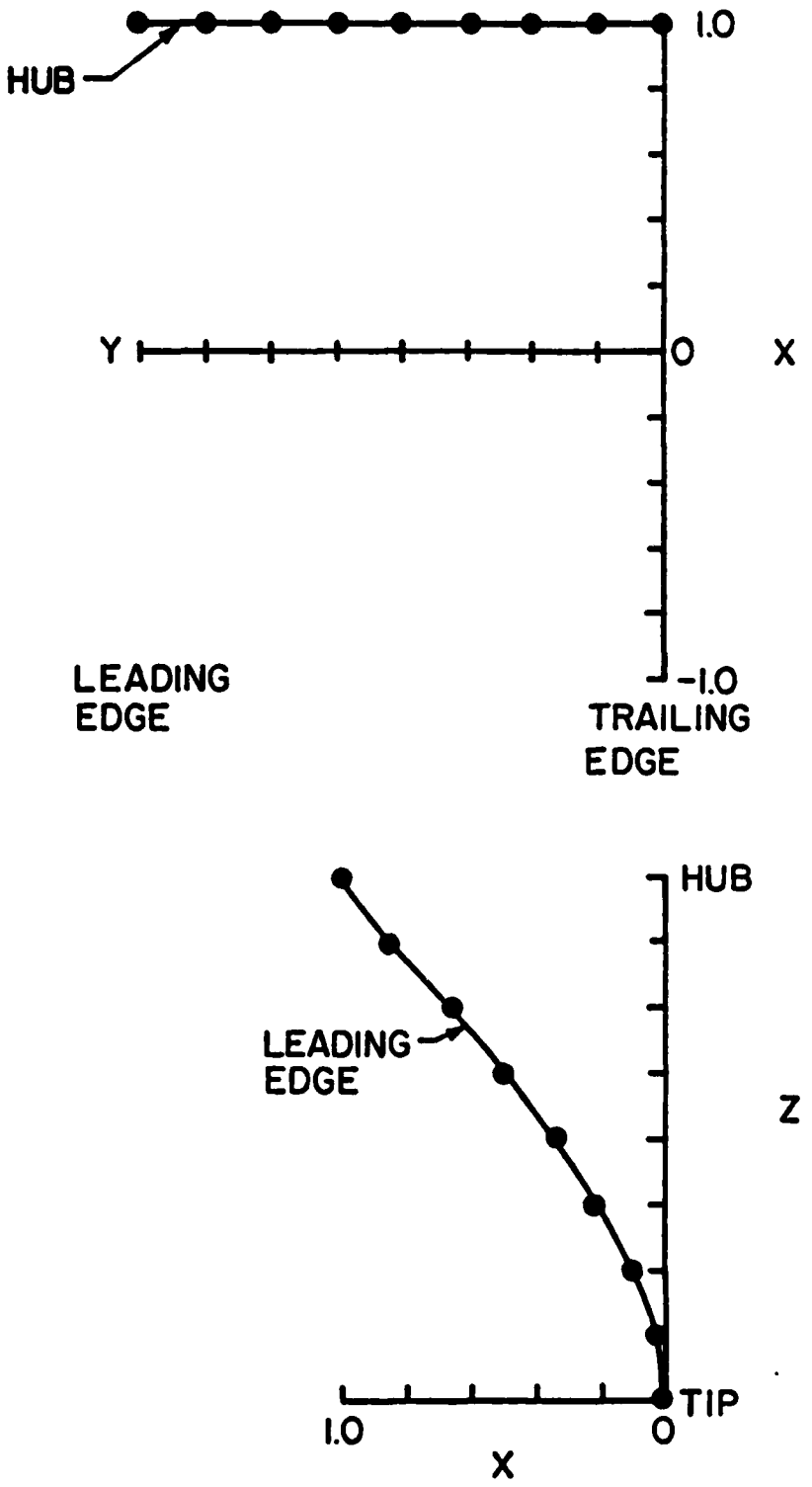

FREQUENCY: 576.4 Hz, 1st BENDING

Figure 5. Predicted Stator Vane First Bend Mode Shape.

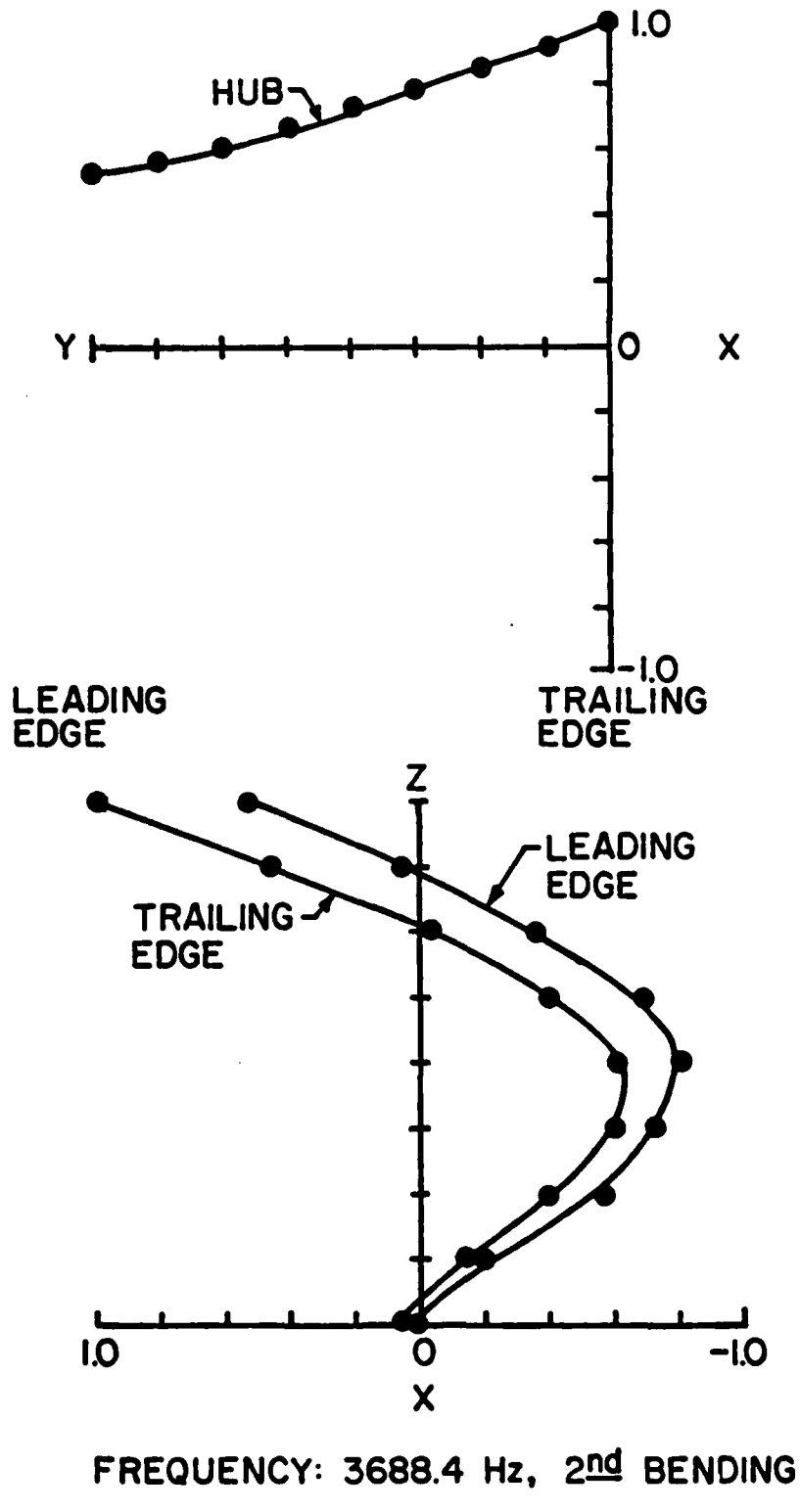

Figure 6. Predicted Stator Vane Second Bend Mode Shape.

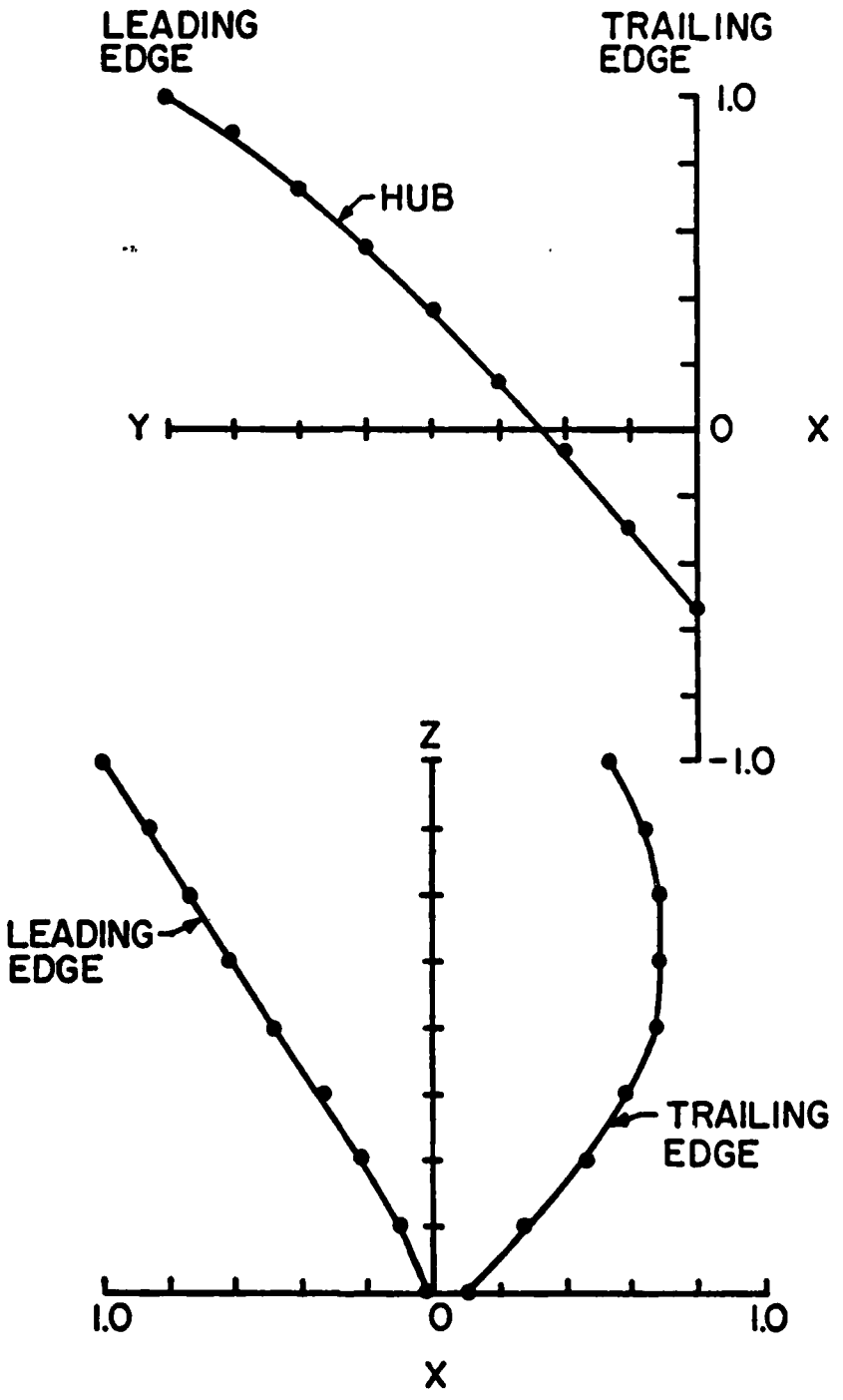

FREQUENCY: 2607.3 Hz, 1st TORSION

Figure 7. Predicted Stator Vane First Torsion Mode Shape.

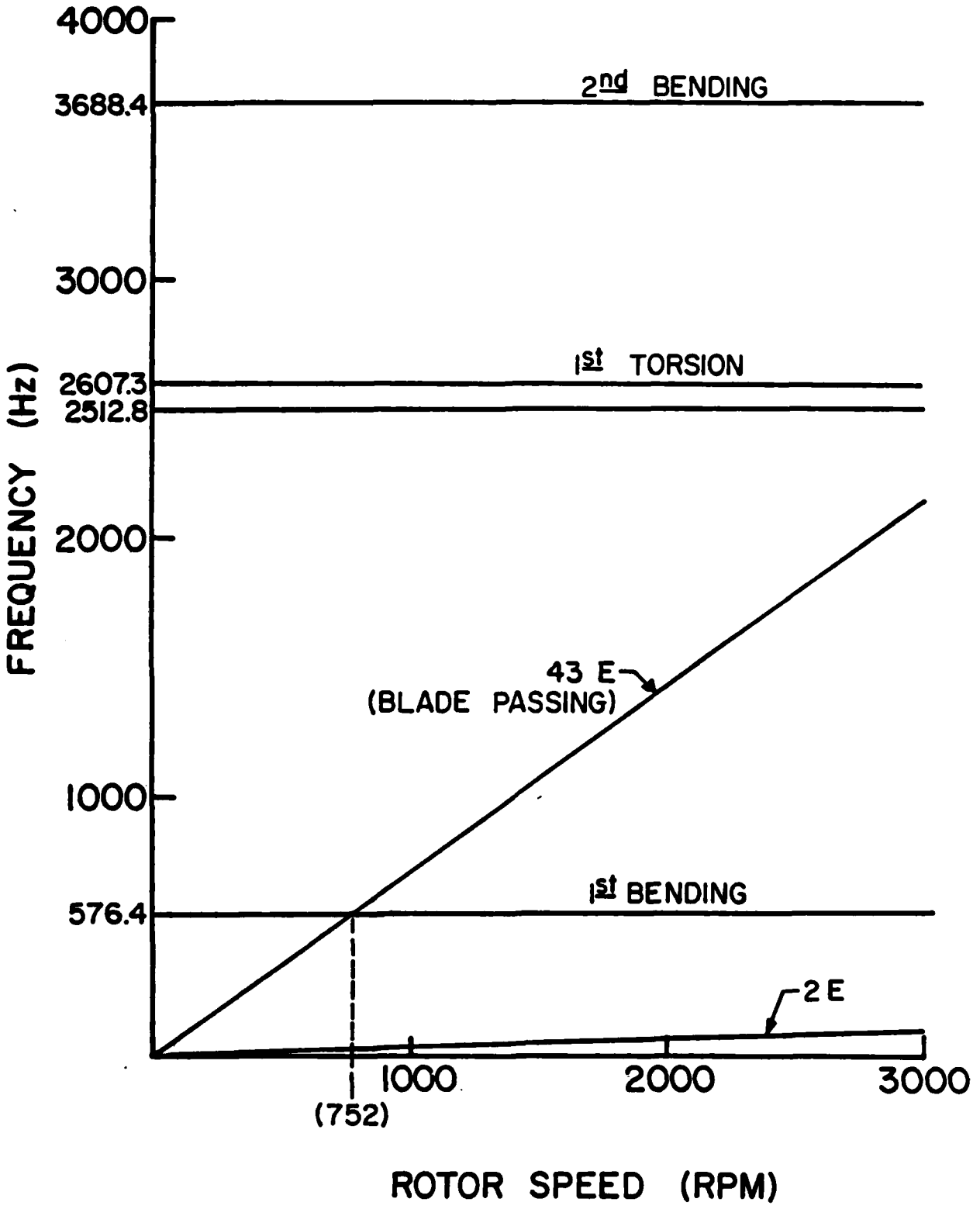

Figure 8. Predicted First Stage Vane Campbell Diagram.

* Dynamic Data Acquisition and Analysis System

In this investigation, both steady and time-variant data will be acquired. Figure 9 presents a schematic of the complete data acquisition and analysis system including the interactions between the steady and the time-variant systems.

The steady-state data acquisition and analysis system is centered around the HP-85 computer seen in Figure 10. These steady-state data will define the points of compressor operation, in terms of overall and stage pressure ratios and corrected mass flow rate, at which the unsteady velocity and surface pressure measurements will be obtained.

The dynamic data acquisition and analysis system has been specified and is currently being made operational. This system is centered around a PDP 11/23 computer and an A-D multiplexer system capable of digitizing signals simultaneously at rates of up to 5 megahertz per channel, also seen in Figure 10.

The time-variant quantities of fundamental interest include the fluctuating aerodynamic forcing function and the resulting chordwise and spanwise distributions of the complex time-variant pressure distributions of the downstream blade and vane rows.

The airfoil surface dynamic pressure measurements are being accomplished with miniature high-response Kulite thin-line design dynamic pressure transducers. Initially pairs of first stage stator vanes are being instrumented such that both the chordwise

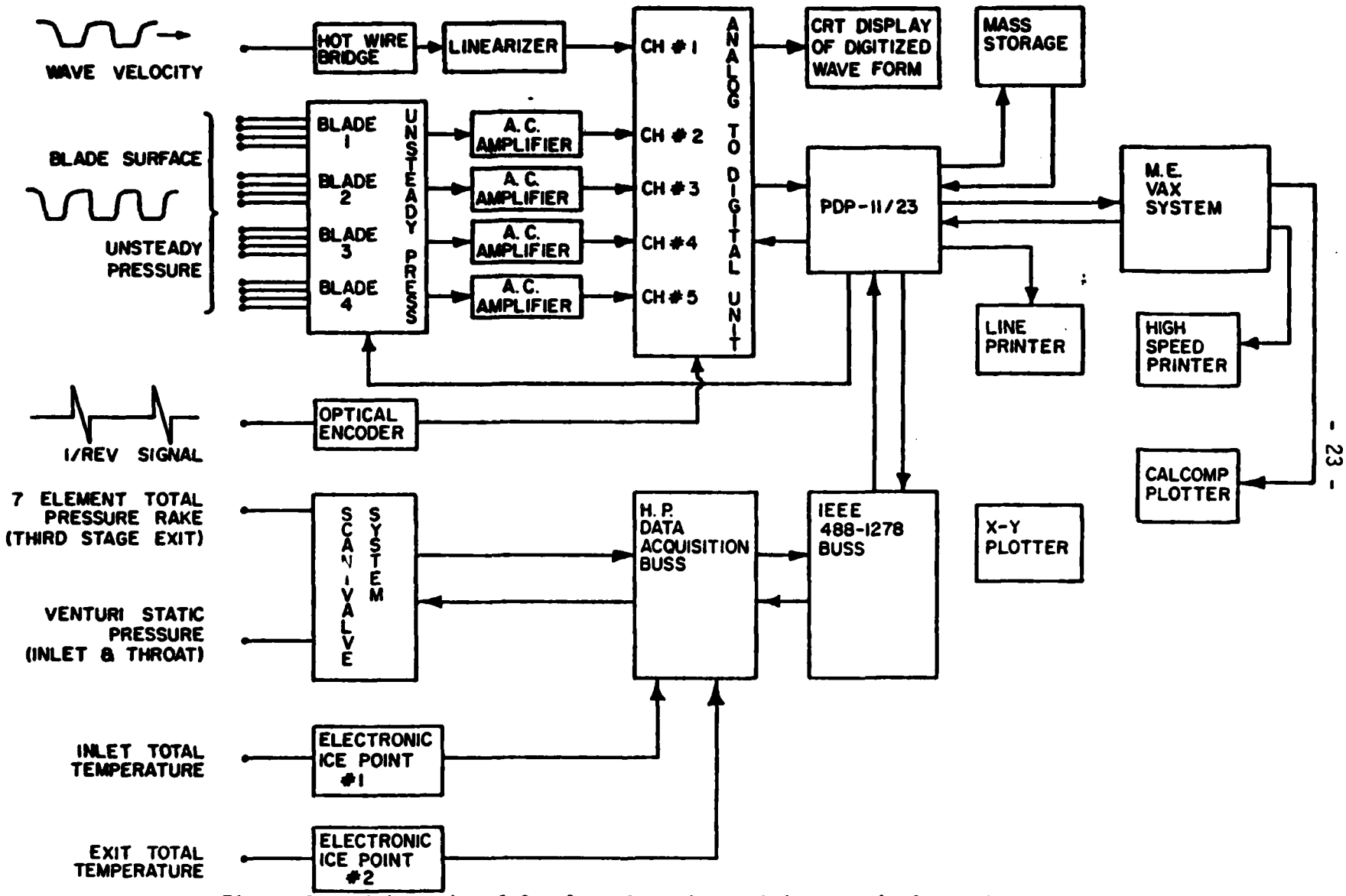

Figure 9. Schematic of Complete Data Acquisition and Analysis System.

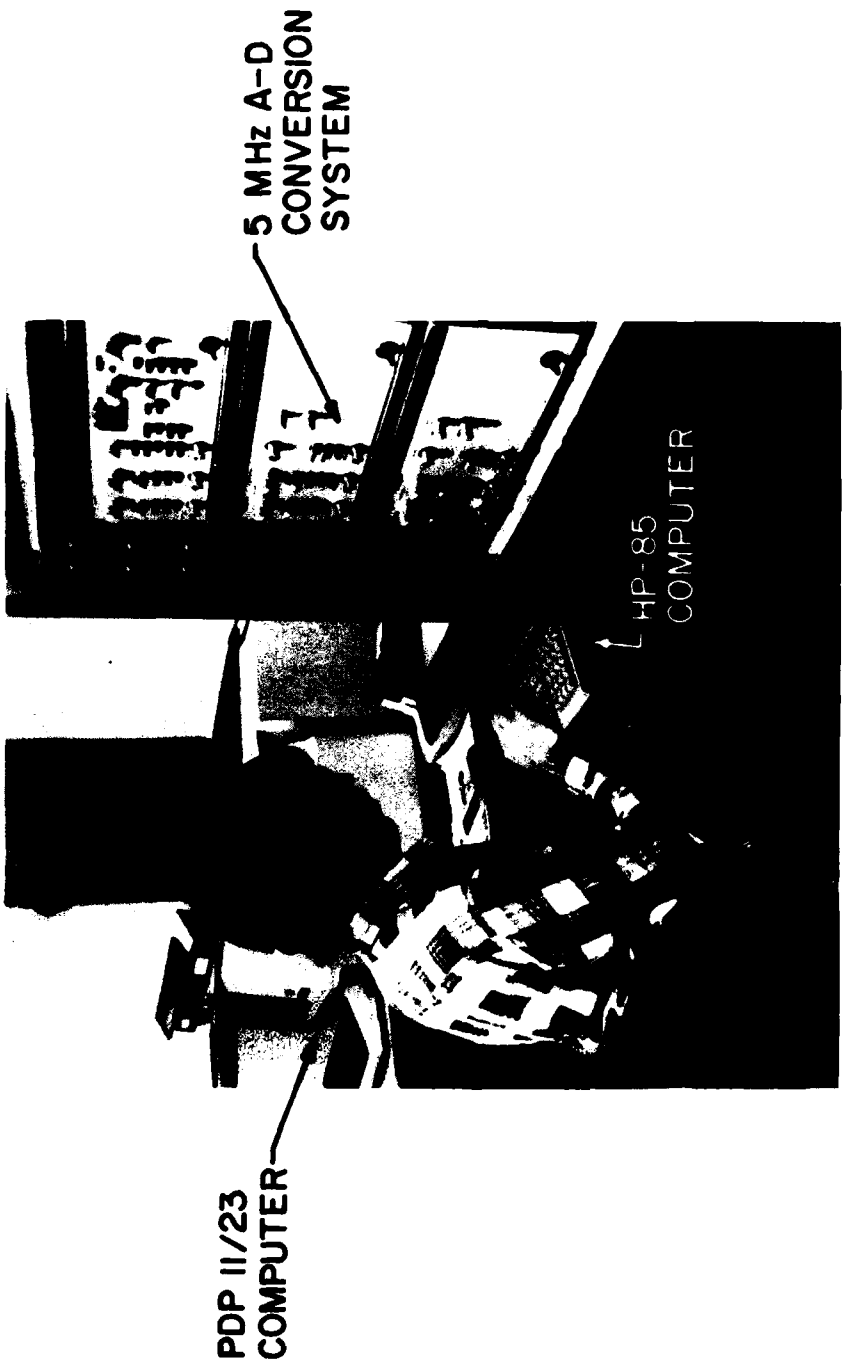

Figure 10. Facility Computer and A-D Conversion Systems.

and spanwise time-variant pressure distributions can be quantitatively determined in one flow passage. It sould be noted that the multi-stage investigation will be accomplished by interchanging the aft stage vane rows with the instrumented first stage vane row. Hence, it is only necessary to instrument this first stage vane row.

The time-variant wake measurements will be obtained by means of a calibrated and linearized cross-wire probe. The probe will be located at mid-stator circumferential spacing with axial location corresponding to mid rotor-stator axial gap in a passage adjacent to the pressure instrumented one. The probe will be traversed radially, thereby defining the time-variant wake at the locations corresponding to the vane or blade surface spanwise dynamic pressure measurements. The mean absolute flow angle will be determined by rotating the probe until a zero voltage difference is obtained between the two hot-wire channnels. This mean angle will then be used as a reference for calculating the instantaneous absolute and relative flow angles. The output from each channel will be corrected for tangential cooling effects and the individual fluctuating velocity components parallel and normal to the mean flow angle calculated from the corrected quantities.

* Data Analysis and Calibration Techniques

The time-variant data acquisition and analysis technique which will be used is based on a data averaging or signal enhancement concept. The key to such a technique is the ability to sample data at a pre-set time. In this investigation the data of interest are being generated at the blade passing frequency. Hence, the logical choice for the time or data initiation reference is the rotor shaft. For this purpose, an optical encoder delivering a square wave voltage signal having a duration in the microsecond range will be used.

At each steady operating point, an averaged time-variant data set, consisting of the hot-wire and Kulite dynamic pressure transducer signals averaged over N blade passages and M rotor revolutions, will be obtained. Each of these digitized signals will then be Fourier decomposed into its harmonics. From this, both the magnitude of the dynamic data and its phase lag as referenced to the optical encoder pulse will be determined. To then relate the wake generated velocity profiles with the surface dynamic pressures on the instrumented vanes, the rotor exit velocity triangles will be examined.

Figure 11 shows the change in the rotor relative exit velocity which occurs as a result of the presence of the blade. A deficit in the velocity in this relative frame creates a change in the absolute velocity, as indicated. This velocity change is measured with the cross hot wires. From this instantaneous abso-

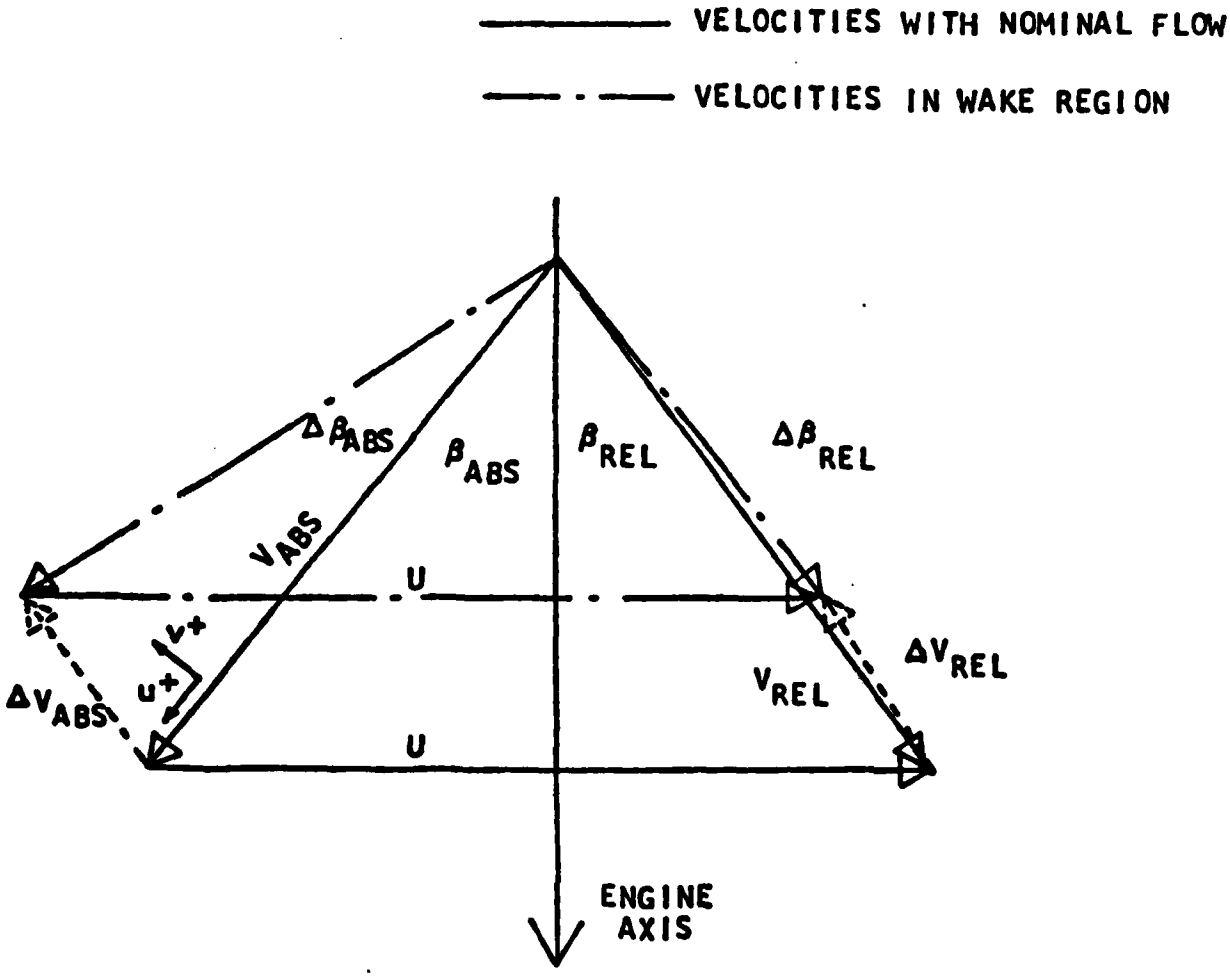

Figure 11. Reduction in relative velocity created by airfoil wake results in corresponding velocity and angular change in absolute frame of reference.

lute angle and velocity, the rotor exit relative angle and velocity and the magnitude and phase of the perturbation quantities will be determined.

As previously noted the cross hot-wire probe will be positioned at mid rotor-stator axial spacing. To relate the time-based events as measured by this hot-wire probe to the unsteady pressures on the vane surfaces, the assumptions are made that: (1) the wakes are identical at the hot-wire and the stator leading edge planes; (2) the wakes are fixed in the relative frame. Figure 12 presents a schematic of the rotor wakes, the instrumented vanes, and the hot-wire probe. The rotor blade spacing, the vane spacing, the length of the probe, and the axial spacing between the vane leading edge plane and the probe holder centerline are known quantities. The hot-wire data will be analyzed to yield the absolute flow angle and the rotor exit relative flow angle. Using the two assumptions noted, the wake can be located relative to the hot-wires and the leading edges of the instrumented van suction and pressure surfaces. From this, the times at which the wake is present at various locations can be determined. The incremented times between occurrences at the hot-wire and the vane leading edge plane can then be related to phase differences between the perturbation velocities and the airfoil surface pressures.

The chordwise and spanwise distributions of the pressure difference on an equivalent single airfoil can then be calculated. These data, as well as the individual surface pressure

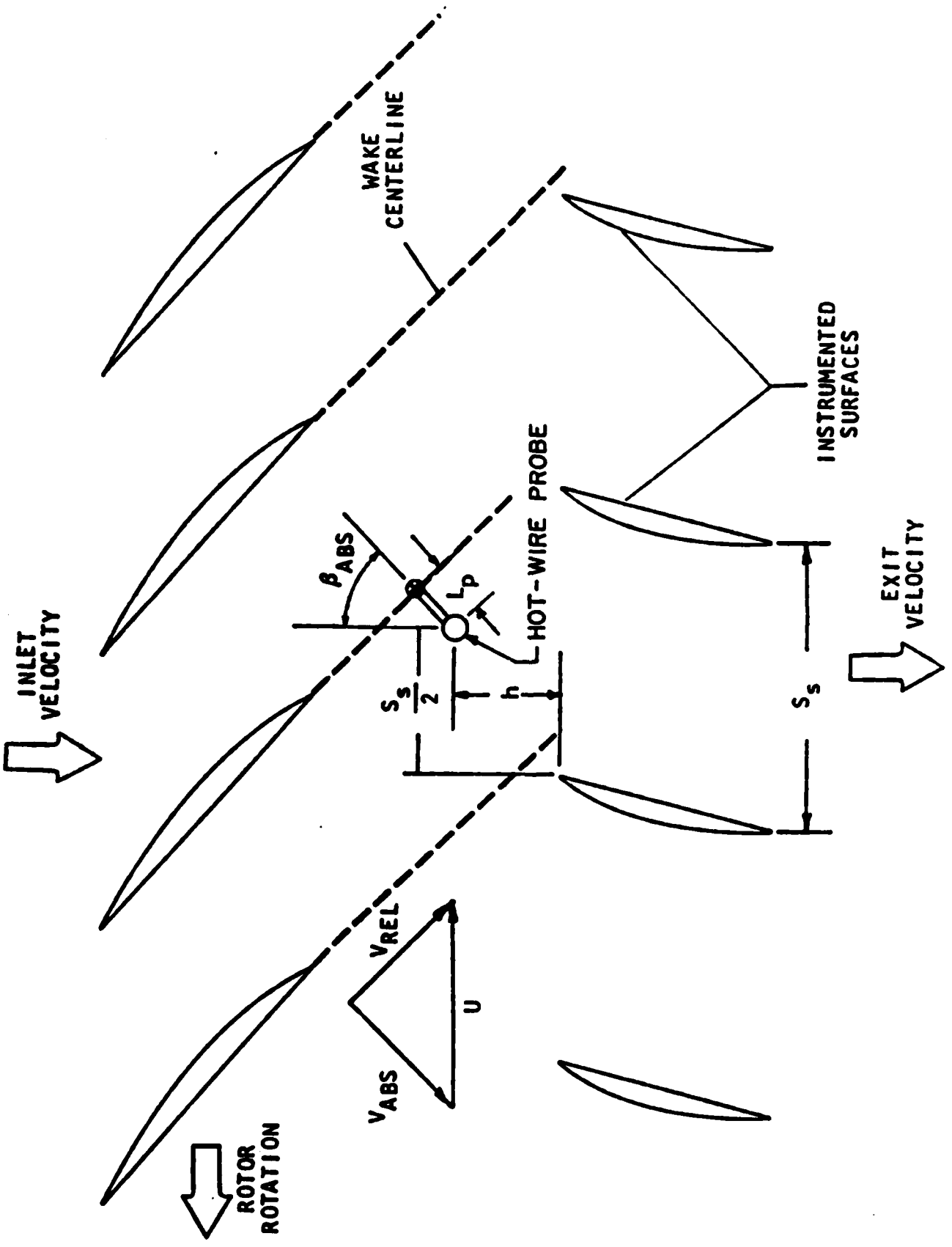

Figure 12. Schematic of flow field utilized in dynamic data analysis.

data, will be normalized with respect to the quantity $\rho \cdot V^2 \cdot \frac{v}{V}$; where ρ is the density, V is absolute velocity, and v the transverse perturbation velocity at the airfoil leading edge. These unsteady pressure differential data will then be correlated with predictions obtained from an appropriate state-of-the-art unsteady aerodynamic cascade analysis.

To obtain accurate time-variant pressure data from surface mounted Kulite transducers, it is imperative that the mounted transducers be dynamically calibrated over the frequency range of interest. Also, it is generally necessary to experimentally determine the distortion of the unsteady pressure signal associated with the specific airfoil surface transducer mounting configuration. For example, to minimize the disturbance to the airfoil contour, the transducer may be mounted from the backside of the airfoil, sensing the unsteady pressure via a small volume inside the airfoil and a static pressure tap on the airfoil surface of interest, as per the airfoil instrumentation of this program. Another example would include placing a thin layer of RTV over the flush mounted transducer for protection. In any event, the distortion of the unsteady pressure signal must be experimentally quantified.

To experimentally determine the transfer function for a dynamic pressure transducer system, a time-variant pressure calibration system is required. Conceptually, the simplest and most direct calibration system involves an harmonic pressure generator. The calibration system of interest herein is based on a

fluidic oscillator, which offers the potential of generating harmonic presssure signals at relatively high frequency values.

A fluidic oscillator, shown schematically in Figure 13, is a bi-stable device that results in a fluid jet oscillating between two output ports. The time duration of the jet in each output port, and thus the oscillator output frequency, is a function of both the fluid density and the length of the feedback line which connects the output and control ports. As the fluid density and the feedback line length decreases, the frequency of oscillation increases. It should be noted that as the frequency is increased, the magnitude of the output signal is decreased. This is not a significant problem and, in fact, can be eliminated by placing a fluidic amplifier in series with the fluidic oscillator.

A calibration rig has been designed, fabricated, and utilized to determine the transfer function for two dynamic total pressure probe-transducer systems with 90° bends and remote transducers, Figure 14, over a frequency range up to 3,000 Hz and correlated with predictions from the Bergh-Tijdeman analysis. Based on the solution of the linearized, compressible Navier-Stokes equations, this analysis predicts the dynamic distortion associated with a pressure tap-tubing-transducer system.

Figure 15 presents the correlation of the experimentally determined transfer function and the corresponding predictions for a probe-transducer system which has a single resonance value

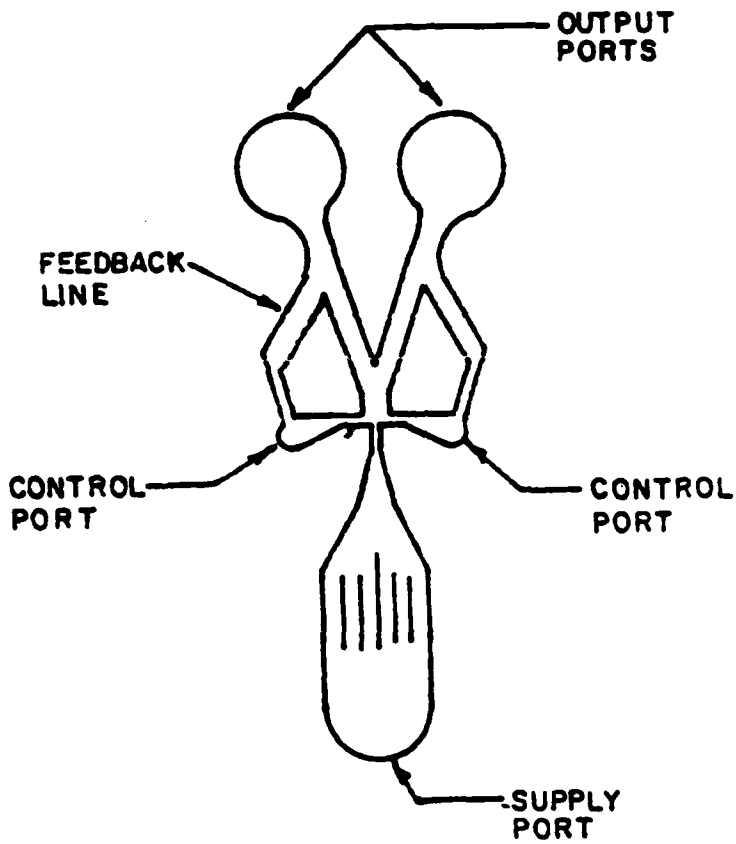

Figure 13. Schematic of Fluidic Oscillator.

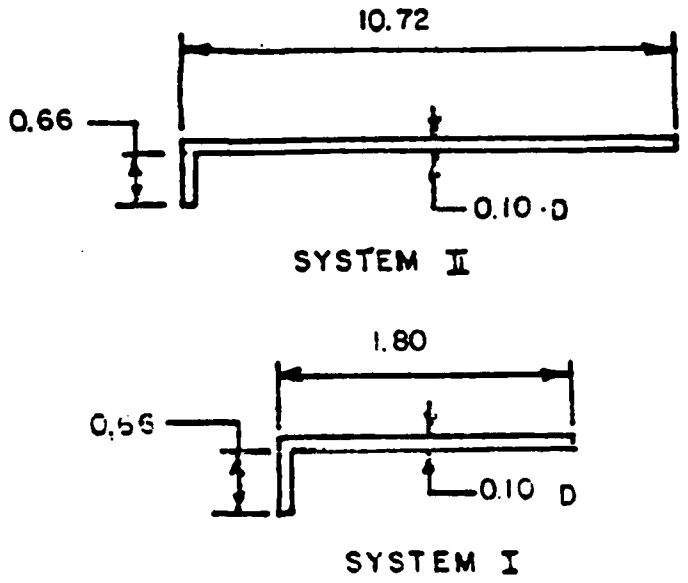

Figure 14. Dynamic Total Pressure Probe-Transducer System Configuration.

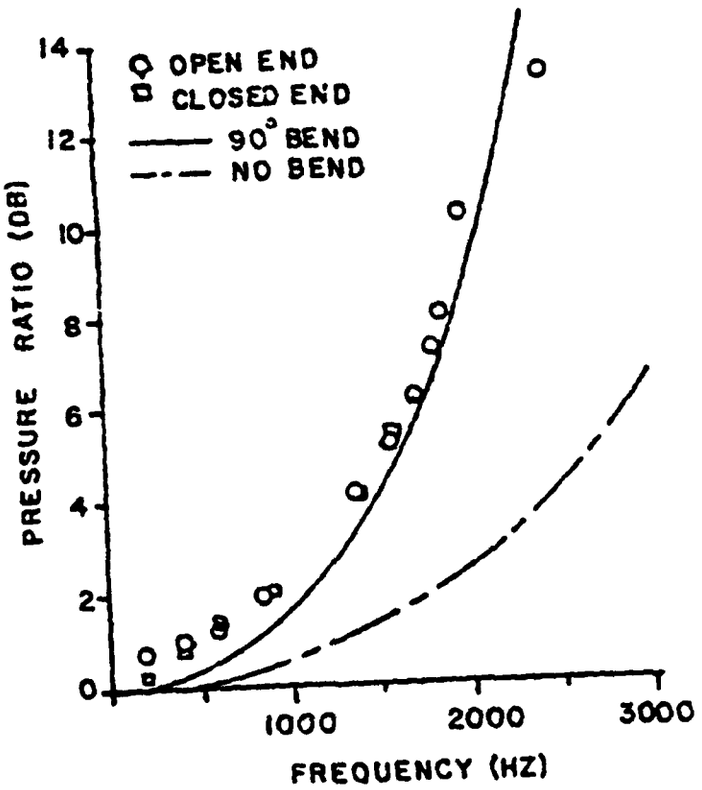

Figure 15. Probe-Transducer System I Transfer Function.

in the frequency range considered. As seen, this data-analysis correlation is very good when the very small 90^{o} bend volume and associated bend length is considered in the analysis. However, when this relatively small 90^{o} bend volume and associated length is neglected, the experiment-analysis correlation is less than satisfactory. Thus, this figure demonstrates the viability of the fluidic oscillator based dynamic pressure calibration system, the validity of the analysis, and the sensitivity of the analysis to relatively small variations in the system geometry.

* Energy Balance Applied to Coupled Aeroelastic Response

The mathematical development of a coupled mode blade vibration structural dynamics model based on an energy balance technique has been completed. In this technique, the energy input to the airfoil system per cycle of oscillation is generated by gust forces and moments and, under certain conditions, the self-induced aerodynamic forces and moments. The energy dissipation per cycle is associated with the structural damping, the static moment term for coupled motions, and under certain conditions, the self-induced aerodynamic forces and moments.

The effects of the various aerodynamic parameters on the coupled mode forced response of a representative airfoil have also been considered. In particular, the effects of the inlet Mach number, the interblade phase angle, the level of structural damping, and the cascade geometry on the coupled bending-torsion

aerodynamically forced response of a flat plate airfoil cascade have been investigated.

A complete and detailed description of this unique model has been presented as AIAA Paper No. 83-0844 and published in the Conference Proceedings of the 24th AIAA/ASME/ASCE/AHS Structures, Structural Dynamics and Materials Conference. This paper is reproduced herein in the Appendix.

APPENDIX

THE COUPLED AEROELASTIC RESPONSE OF TURBOMACHINERY BLADING TO AERODYNAMIC EXCITATIONS

AIAA Paper No. 83-0844

Conference Proceedings

24th AIAA/ASME/ASCE/AHS

Structures, Structural Dynamics and Materials Conference

May 1983

83-0844

THE COUPLED AEROELASTIC RESPONSE OF TURBOMACHINERY BLADING TO AERODYNAMIC EXCITATIONS

Daniel Hoyniak* and Sanford Fleeter**
Thermal Sciences and Propulsion Center
School of Mechanical Engineering
Purdue University
West Lafayette, Indiana 47907

Abstract

An energy balance technique is developed to predict the coupled bending-torsion mode aerodynamically forced response of an airfoil. In this technique, the energy input to the airfoil system per cycle of oscillation is generated by gust forces and moments and, under certain conditions, the self-induced aerodynamic forces and moments. The energy dissipation per cycle is associated with the structural damping, the static moment term for coupled motions, and under certain conditions, the self-induced aerodynamic forces and moments. The effects of the various aerodynamic parameters on the coupled forced response are then considered. In particular, the effects of the inlet Mach number, the interblade phase angle, the level of structural damping, and the cascade geometry on the coupled bending-torsion aerodynamically forced response of a flat plate airfoil cascade are demonstrated.

Nomenclature

a	dimensionless distance of elastic axis aft of mid-chord
b	1/2 airfoil chord (C/2)
g	structural damping coefficient
h	complex translational motion
h_o	amplitude of translational oscillation
i	$\sqrt{-1}$
k	reduced frequency ($k = \bar{\omega}b/U$)
m	mass per unit span of the airfoil
r_α	radius of gyration about elastic axis
x_α	location of center of gravity relative to elastic axis
A	unsteady lift influence coefficient
B	unsteady moment influence coefficient
C	airfoil chord
C/S	cascade solidity (airfoil chord/airfoil spacing)

$$C_1 = \mu x_\alpha + (A_\alpha)^R$$

$$C_2 = \mu x_\alpha + (B_h)^R$$

$$C_3 = \left(\mu - \mu\left(\frac{\omega_h}{\bar{\omega}}\right)^2 + (A_h)^R\right)$$

$$C_4 = (A_h)^I - \mu\left(\frac{\omega_h}{\bar{\omega}}\right)^2 g_h$$

$$C_5 = \mu r_\alpha^2 \left(1 - \left(\frac{\omega_\alpha}{\bar{\omega}}\right)^2\right) + (B_\alpha)^R$$

$$C_6 = (B_\alpha)^I - \mu r_\alpha^2 \left(\frac{\omega_\alpha}{\bar{\omega}}\right)^2 g_\alpha$$

$$C_7 = -\left(\frac{W_G}{U}\right)(A_G)^R$$

$$C_8 = -\left(\frac{W_G}{U}\right)(A_G)^I$$

$$C_9 = -\left(\frac{H_G}{U}\right)(B_G)^R$$

$$C_{10} = -\left(\frac{W_G}{U}\right)(B_G)^I$$

$$D_R = [(C_3C_5 - C_4C_6) - (C_2C_1 - (A_\alpha)^I(B_h)^I)]$$

$$D_I = [(C_4C_5 + C_6C_3) - (C_2(A_\alpha)^I + C_1(A_h)^I)]$$

I_α	mass moment of inertia per unit span about the elastic axis
L	unsteady lift
M	unsteady moment

$$N_{hR} = [(C_7C_5 - C_8C_6) - (C_1C_9 - C_{10}(A_\alpha)^I)]$$

$$N_{hI} = [(C_8C_5 + C_6C_7) - (C_9(A_\alpha)^I + C_1C_{10})]$$

$$N_{\alpha R} = [(C_3C_9 - C_4C_{10}) - (C_7C_2 - C_8(B_h)^I)]$$

$$N_{\alpha I} = [(C_{10}C_3 + C_4C_9) - (C_7(B_h)^I + C_2C_8)]$$

Re [ ]	real part of [ ]
S_α	airfoil static moment per unit span about the elastic axis
U	free-stream velocity
WORK	unsteady work per cycle of oscillation
W	complex transverse gust function
W_G	amplitude of transverse gust
α	complex torsional motion
α_o	amplitude of torsional motion
μ	mass parameter
ρ	fluid density
σ	interblade phase angle
ω	airfoil natural frequency
$\bar{\omega}$	frequency of the transverse gust

* Presently, Aerospace Engineer, NASA-Lewis Research Center, Cleveland, Ohio
** Professor of Mechanical Engineering and Director, Thermal Sciences and Propulsion Center Member AIAA

Subscripts

G	gust
SI	self-induced
h	translation
α	torsion

Superscripts

I	imaginary part
R	real part
·	derivative with respect to time

Introduction

Aerodynamically induced vibrations of rotor and stator airfoils are one of the more common sources of high cycle fatigue failure in gas turbine engines. Destructive aerodynamic forced responses of fan, compressor, and turbine blading have been generated by a wide variety of sources including upstream blades and/or vanes, distortion, rotating stall, downstream blades and/or vanes, surge, bleeds, and random or otherwise unidentified sources.

Failure level vibratory responses occur when a periodic aerodynamic forcing function, with frequency equal to a natural blade resonant frequency, acts on a blade row. The rotor speeds at which these forced responses occur are predicted with Campbell diagrams which display the natural frequency of each blade mode versus rotor speed.[1] Whenever these curves cross, aerodynamically induced forced responses are possible. However, no accurate prediction for the amplitude of the resulting stress can currently be made.

Because it is rarely, if ever, possible to eliminate all vibration excitation from the operating range of turbomachine blade rows, and not possible to accurately predict the amplitude of the stresses with present day technology, the resonant stresses are not known until the first build-up test of engine components. When excessive stresses or failures are then discovered, an extensive and costly re-design, re-build, and re-test program is necessary in order to effect a viable solution.

The accurate first principles prediction of the aerodynamically forced response of a blade or vane involves the following elements. Spatially periodic variations in pressure, velocity, and flow direction of the exit flow field of an upstream element appear as temporally varying in a coordinate system fixed to the downstream row. As a result, individual airfoils are subject to a time-varying aerodynamic forcing function which can induce high vibratory stress levels.

The prediction of the aerodynamically forced response vibratory behavior of a blade or vane row requires a definition of the unsteady forcing function in terms of its harmonics. The time-variant aerodynamic response of the airfoil to each harmonic of this forcing function is then assumed to be comprised of two parts.[2] One is due to the disturbance being swept past the non-responding fixed airfoils. The second arises when the airfoils respond to this disturbance. These effects are modeled by means of two distinct analyses. A linearized small perturbation gust analysis is used to predict the time-variant aerodynamics of the fixed non-responding airfoil to each harmonic of the disturbance. A self-induced unsteady aerodynamic analysis wherein the airfoils are assumed to be harmonically oscillating is then used to predict the additional aerodynamic effect due to the airfoil response. Reviews of the state-of-the-art of unsteady aerodynamics as applied to turbomachines, including gust and self-induced unsteady aerodynamic analyses, are presented in references 3 and 4.

The classical approach for the prediction of the aerodynamically forced response of an airfoil is based on Newton's second law. The gust and self-induced unsteady aerodynamic analyses are used to describe the harmonic forces and moments acting on the airfoil in conjunction with a lumped parameter description of the airfoil structural and inertial properties.[5]

An alternative approach based on an energy balance technique has been developed by Hoyniak and Fleeter[6] to predict the uncoupled single-degree-of-freedom forced response of an airfoil. In this approach, an energy balance is conducted between the unsteady aerodynamic work and the energy dissipated by the airfoil.

The objectives of the research described in this paper include the extension of the energy balance technique to include the more realistic case of coupled bending-torsion mode forced response of an airfoil, and the subsequent demonstration of the effects of the various aerodynamic and structural parameters on this coupled response.

General Unsteady Aerodynamic Coefficients

Figure 1 presents a schematic representation of a two-dimensional airfoil section displaced in both torsion and translation in a uniform flow with a superimposed convected transverse sinusoidal gust. Equations 1 and 2 present the complex, time-dependent unsteady lift and moment per unit span, written in influence coefficient form, for the gust response and the self-induced aerodynamic cases respectively.

$$\left.\begin{aligned} L_G &= L_G^R + iL_G^I = \pi\rho b^{3-2}\omega^{-2}\,[A_G(\tfrac{W}{U})] \\ M_G &= M_G^R + iM_G^I = \pi\rho b^{4-2}\omega^{-2}\,[B_G(\tfrac{W}{U})] \end{aligned}\right\} \quad (1)$$

$$\left.\begin{aligned} L_{SI} &= L_{SI}^R + iL_{SI}^I = \pi\rho b^3\omega^2\,[A_h\,h + A_\alpha\alpha] \\ M_{SI} &= M_{SI}^R + iM_{SI}^I = \pi\rho b^4\omega^2\,[B_h\,h + B_\alpha\alpha] \end{aligned}\right\} \quad (2)$$

where: $h = h_o e^{i\omega t}$; $\alpha = \alpha_o e^{i\omega t}$; and

$W = W_G e^{i\bar{\omega}t}$ describes the gust; (A_h, B_h), (A_α, B_α), (A_G, B_G) denote the generalized unsteady lift and moment coefficients due to airfoil translation, airfoil torsion, and the convected sinusoidal gust, respectively; ω is the airfoil natural frequency, and $\bar{\omega}$ is the gust forcing function frequency.

The total unsteady lift and moment on the airfoil are obtained by superimposing the gust response and the self-induced aerodynamic forces and moments.

$$L(t) = L_G(t) + L_{SI}(t) = \pi\rho b^{3-2}\omega^2 \left[A_G\left(\frac{W_G}{U}\right) + A_h\, h_o + A_\alpha\, \alpha_o\right] e^{i\bar{\omega}t}$$

$$M(t) = M_G(t) + M_{SI}(t) = \pi\rho b^{4-2}\omega^2 \left[B_G\left(\frac{W_G}{U}\right) + B_h\, h_o + B_\alpha\, \alpha_o\right] e^{i\bar{\omega}t} \qquad (3)$$

It should be noted that the airfoil response occurs at the frequency of the forcing function. Hence the gust frequency, $\bar{\omega}$, has been utilized in the specification of the unsteady aerodynamic forces and moments, Equation 3.

Energy Balance

The equations of motion describing the coupled translational and torsional displacement of the flat plate airfoil depicted in Figure 1 are given in Equation 4.

$$m\ddot{h} + S_\alpha\ddot{\alpha} + m\omega_h^2(1 + ig_h)h = L(t)$$

$$S_\alpha\ddot{h} + I_\alpha\ddot{\alpha} + I_\alpha\omega_\alpha^2(1 + ig_\alpha)\alpha = M(t) \qquad (4)$$

where m denotes the mass per unit span of the airfoil, S_α is the airfoil static moment per unit span about the elastic axis, ω_h and ω_α are the translational and torsional mode airfoil natural frequencies of the corresponding undamped single-degree-of-freedom system respectively, and I_α is the mass moment of inertia per unit span about the elastic axis. As seen, the airfoil structural dynamic system described by Equation 4 is strongly coupled, with this coupling associated with both the structural and the aerodynamic characteristics of the system. The structural coupling becomes significant whenever the aerodynamic center does not coincide with the elastic axis, thereby resulting in a non-zero value for the airfoil static moment. The aerodynamic coupling arises because the self-induced aerodynamic forces acting on the airfoil are a function of the translational and torsional motions.

In this investigation, the coupled system response is determined utilizing an energy balance technique. The energy input to the system per cycle of airfoil oscillation is generated by the gust and, under certain conditions, the self-induced aerodynamic forces and moments.[6] The energy dissipation of the system per cycle is associated with the system structural damping, under certain conditions the self-induced aerodynamic forces and moments, and the static moment term, S_α. It should be noted that for the uncoupled single-degree-of-freedom case, the dissipation term, S_α, is not considered.

This energy balance for the coupled translation-torsion airfoil motion can be expressed as follows.

$$(WORK)^h_{SI} + (WORK)^h_{g_h} + (WORK)^h_{S_\alpha} = (WORK)^h_G$$

$$(WORK)^\alpha_{SI} + (WORK)^\alpha_{g_\alpha} + (WORK)^\alpha_{S_\alpha} = (WORK)^\alpha_G \qquad (5)$$

where:

$(WORK)^h_{SI}$, $(WORK)^\alpha_{SI}$ = work done by the self-induced aerodynamic forces and moments in translation and torsion, respectively.

$(WORK)^h_{g_h}$, $(WORK)^\alpha_{g_\alpha}$ = work done by the airfoil translation and torsion structural damping, respectively.

$(WORK)^h_{S_\alpha}$, $(WORK)^\alpha_{S_\alpha}$ = work associated with the static moment, S_α, in translation and torsion, respectively.

$(WORK)^h_G$, $(WORK)^\alpha_G$ = work done by the gust aerodynamic forces and moments in translation and torsion, respectively.

It should be noted that the work associated with the self-induced aerodynamic forces and moments, $(WORK)^h_{SI}$ and $(WORK)^\alpha_{SI}$, have been written as dissipation terms. However, under certain conditions they may actually represent energy input terms. Mathematically, this is accounted for based on the sign of these work terms. Also, matrix techniques will be utilized to solve Equation 5 in order to determine the motion of the airfoil system.

The unsteady work done by the self-induced aerodynamic terms, $(WORK)^h_{SI}$ and $(WORK)^\alpha_{SI}$, over one cycle of vibration can be calculated from Equation 6.

$$(WORK)^h_{SI} = -\oint \mathrm{Re}[L_{SI}(t)\, dh]$$

$$(WORK)^\alpha_{SI} = \oint \mathrm{Re}[M_{SI}(t)\, d\alpha] \qquad (6)$$

where $L_{SI}(t)$ and $M_{SI}(t)$ denote the unsteady lift and moment associated with the self-induced harmonic motion of the airfoil, per Equation 2. Also, the negative sign associated with the aerodynamic lift integral of Equation 6 is a result of the standard aeroelastic convention that positive lift and positive translational displacement are defined in opposite directions.

Carrying out the integrations specified by Equations 2 and 6 results in the following expressions for the unsteady work done by the self-induced aerodynamic forces and moments.

$$(WORK)^h_{SI} = -\pi^2\rho b^3\bar{\omega}^2\left[-(A_h)^I\left(\frac{h_o}{b}\right)^2 + (A_\alpha)^R h_o\alpha_o SIN(\lambda_h-\lambda_\alpha) - (A_\alpha)^I h_o\alpha_o COS(\lambda_h-\lambda_\alpha)\right]$$

$$(WORK)^\alpha_{SI} = -\pi^2\rho b^4\bar{\omega}^2\left[(B_h)^R\left(\frac{h_o\alpha_o}{b}\right)SIN(\lambda_h-\lambda_\alpha) - (B_h)^I\left(\frac{h_o\alpha_o}{b}\right)COS(\lambda_h-\lambda_\alpha) - (B_\alpha)^I\alpha_o^2\right] \quad (7)$$

The angle λ_h denotes the phase angle between the incoming gust and the resulting translational motion of the airfoil. Similarly, the angle λ_α is the phase angle between the incoming gust and the airfoil torsional motion.

The energy input to the airfoil is determined by calculating the work per cycle of oscillation of the unsteady lift and moment associated with the incoming gust.

$$(WORK)^h_G = -\oint Re[L_G(t)dh]$$
$$(WORK)^\alpha_G = \oint Re[M_G(t)d\alpha] \quad (8)$$

Again, the negative sign is included in the lift integral as a result of the differences in the definitions of positive lift and positive translational displacement.

The evaluation of these integrals, Equations 8 and 2, yields the following for the gust work.

$$(WORK)^h_G = -\pi\rho b^3\bar{\omega}^2 h_o\left[(A_G)^I COS(\lambda_h) - (A_G)^R SIN(\lambda_h)\right]$$
$$(WORK)^\alpha_G = \pi\rho b^4\bar{\omega}^2\alpha_o\left[(B_G)^I COS(\lambda_\alpha) - (B_G)^R SIN(\lambda_\alpha)\right] \quad (9)$$

The energy dissipated by the structural damping over one cycle of oscillation can be calculated as follows.

$$(WORK)^h_{g_h} = \oint Re[ig_h m\omega_h^2 h dh]$$
$$(WORK)^\alpha_{g_\alpha} = \oint Re[ig_\alpha I_\alpha\omega_\alpha^2\alpha d\alpha] \quad (10)$$

Carrying out the integrations yields the following:

$$(WORK)^h_{g_h} = \pi g_h m\omega_h^2 h_o^2$$
$$(WORK)^\alpha_{g_\alpha} = \pi g_\alpha I_\alpha\omega_\alpha^2\omega_o^2 \quad (11)$$

The unsteady work associated with the static moment, S_α, merits some additional comment. This is the term which couples the system equations of motion when the elastic axis and the aerodynamic center do not coincide. Physically, the S_α term can be considered as either a torsional force applied to the airfoil as the result of a unit translation airfoil displacement or as a translational force resulting from the application of a unit torsional displacement. Thus, for an airfoil undergoing a translation mode oscillation, there is an apparent torsional load that can either do work on or extract work from the airfoil system. The phase relationship between the translational and torsional displacement determines whether this apparent torsional load adds or dissipates energy in the airfoil system.

The unsteady work per cycle of oscillation associated with the static moment can be determined per Equation 12.

$$(WORK)^h_{S_\alpha} = \oint Re[S_\alpha\ddot{\alpha}dh]$$
$$(WORK)^\alpha_{S_\alpha} = \oint Re[S_\alpha\ddot{h}d\alpha] \quad (12)$$

The evaluation of these integrals leads to the following.

$$(WORK)^h_{S_\alpha} = S_\alpha\bar{\omega}^2\alpha_o h_o\,\pi\,SIN(\lambda_h-\lambda_\alpha)$$
$$(WORK)^\alpha_{S_\alpha} = S_\alpha\bar{\omega}^2\alpha_o h_o\,\pi\,SIN(\lambda_\alpha-\lambda_h) \quad (13)$$

As previously noted, the sign of the work associated with the static moment is determined by the phase relationship between the translational and torsional displacements per Equation 13.

The substitution of the various work expressions, Equations 7, 9, 11, and 13, into the energy balance, Equation 5, yields the following matrix expression for the coupled translational and torsional airfoil displacements.

$$\begin{bmatrix} A_{11} & A_{12} \\ A_{21} & A_{22} \end{bmatrix}\begin{bmatrix} \left(\frac{h_o}{b}\right) \\ (\alpha_o) \end{bmatrix} = \begin{bmatrix} B_{11} \\ B_{21} \end{bmatrix} \quad (14)$$

where:

$$A_{11} = [\pi g_h m\omega_h^2 b] + [(A_h)^I\pi^2\rho b^3\bar{\omega}^2]$$

$$A_{12} = [S_\alpha \bar{\omega}^2 \pi - (A_\alpha)^R \pi^2 \rho b^3 \bar{\omega}^2] \mathrm{SIN}(\lambda_h - \lambda_\alpha)$$

$$+[(A_\alpha)^I \pi^2 \rho b^3 \bar{\omega}^2 \mathrm{COS}(\lambda_h - \lambda_\alpha)]$$

$$A_{21} = [S_\alpha \bar{\omega}^2 \pi - (B_h)^R \pi^2 \rho b^4 \bar{\omega}^2] \mathrm{SIN}(\lambda_\alpha - \lambda_h)$$

$$+[(B_h)^I \pi^2 \rho b^4 \bar{\omega}^2 \mathrm{COS}(\lambda_h - \lambda_\alpha)]$$

$$A_{22} = \pi g_\alpha I_\alpha \omega_\alpha^2 + (B_\alpha)^I \pi \rho b^4 \bar{\omega}^2$$

$$B_{11} = -\pi \rho b^3 \bar{\omega}^2 \left(\frac{W_G}{U}\right) [(A_G)^I \mathrm{COS}(\lambda_h) -$$

$$(A_G)^R \mathrm{SIN}(\lambda_h)]$$

$$B_{21} = \pi^2 \rho b^4 \bar{\omega}^2 \left(\frac{W_G}{U}\right) [(B_G)^I \mathrm{COS}(\lambda_\alpha) -$$

$$(B_G)^R \mathrm{SIN}(\lambda_\alpha)]$$

The phase angles between the translational and torsional displacements, λ_h and λ_α respectively, can be determined in various ways. For example, they can be determined directly from the classical solution of the coupled system equations of motion, Equation 4, per reference 5. For convenience and brevity, these phase angle relationships are presented in Equation 15.

$$\lambda_h = \mathrm{TAN}^{-1}\left[\frac{N_{hI} D_R - N_{hR} D_I}{N_{hR} D_R + N_{hI} D_I}\right]$$

$$\lambda_\alpha = \mathrm{TAN}^{-1}\left[\frac{N_{\alpha I} D_R - N_{\alpha R} D_I}{N_{\alpha R} D_R + N_{\alpha I} D_I}\right] \qquad (15)$$

where N_{hI}, $N_{\alpha I}$, N_{hR}, $N_{\alpha R}$, D_R, and D_I are defined in terms of the airfoil structural properties and the unsteady aerodynamic forces and moments in the Nomenclature.

Unsteady Aerodynamic Forces and Moments

L_h, M_h, L_α and M_α denote the standard form for the unsteady aerodynamic forces and moments and represent the unsteady lift and moment in translation and torsion, respectively calculated about the airfoil 1/4 chord. These standard form 1/4 chord coefficients are related to the general unsteady aerodynamic influence coefficients through the following relationships.

$$A_h = L_h$$

$$A_\alpha = L_\alpha - (1/2 + a) L_h$$

$$A_G = L_W$$

$$B_h = M_h - (1/2 + a) L_h \qquad (16)$$

$$B_\alpha = M_\alpha - (1/2 + a)(L_\alpha + M_h) + (1/2 + a)^2 L_h$$

$$B_G = M_W$$

where: a is the dimensionless distance of the torsion axis measured from the airfoil mid-chord, as depicted in Figure 1.

Results

To demonstrate the effects of the various parameters on the coupled forced response of turbomachinery blading, the unsteady aerodynamic analysis of reference 7 will be utilized.

This analysis predicts the gust and self-induced unsteady aerodynamic forces and moments for a cascade of flat plate airfoils at zero incidence in a compressible flow field. The structural properties for this parametric study are based on an airfoil with a 5.08 cm chord, a four percent thickness-to-chord ratio, and an aspect ratio of 3. This representative airfoil has a natural translation mode frequence, ω_h, 12% larger than the natural torsion mode frequency, ω_α. Hence $\omega_h/\omega_\alpha = 1.12$. Specific parameters to be varied include the structural damping value, the cascade solidity, the interblade phase angle, the inlet Mach number, and the elastic axis location. In addition, to clearly demonstrate the coupling effects, the airfoil stiffness is varied so as to make the torsional and translation mode natural frequencies nearly equal in value.

The coupled forced response characteristics of the representative airfoil determined utilizing this energy balance technique are presented as a function of the nondimensional ratio of the gust forcing frequency to the airfoil natural torsion mode frequency, $\bar{\omega}/\omega_\alpha$. Hence, values of 1.00 and 1.12 for this nondimensional frequency ratio correspond to the situations where the forcing function frequency is equal to the natural torsion and translation mode frequencies, respectively, of the representative airfoil. Results presented include the translational amplitude, the torsion mode amplitude, and the phase angles between the aerodynamic forcing function and the resulting airfoil as a function of the nondimensional frequency ratio.

The effect of structural damping on the coupled forced response of this representative airfoil is presented in Figures 2 through 5. Figures 2 and 3 present the translational and torsional responses of the airfoil with structural damping as a parameter when the forcing function frequency is in the neighborhood of the natural torsion mode frequency, ω_α. Similarly, Figures 4 and 5 present the translational and torsional

airfoil responses, respectively, with structural damping as the parameter when the forcing function frequency is near to ω_h.

From these figures it can be seen that increased structural damping results in decreased amplitude of response. It should be noted that the maximum response amplitudes do not occur at frequency ratio values of 1.00 or 1.12 even for the special case of zero structural damping. This is a result of the self-induced unsteady aerodynamic forces which correspond in this case to aerodynamic damping. Thus, even when there is no structural damping in the airfoil sytem, the self-induced aerodynamics can generate aerodynamic damping.

Also as anticipated, and seen in Figures 2 through 5, when the gust forcing function frequency is near to the natural torsion mode frequency, the torsional response amplitude is an order of magnitude greater than the corresponding coupled translation mode response, Figures 2 and 3. Analogously, when the forcing function frequency is in the near vicinity of the natural translation mode frequency, the translational response is an order of magnitude greater than the coupled torsion mode response, Figures 4 and 5. Thus, for the other parameters considered herein, only the coupled forced torsional response will be presented for the forcing function frequency near to the airfoil natural torsional frequency ($\bar{\omega}/\omega_\alpha \approx 1$), and only the coupled forced translational response for forcing function frequencies near the natural translational frequency ($\bar{\omega}/\omega_\alpha \approx 1.12$).

The effects of cascade solidity (C/S) and stagger angle on the coupled forced response amplitudes are shown in Figures 6 and 7 and Figures 8 and 9, respectively. As seen, both the coupled torsional and translational forced response amplitudes increase with increasing values of the solidity and the stagger angle. The variations in the solidity result in a somewhat more pronounced effect on the translational response than on the torsional response, Figures 6 and 7. However, the stagger angle variation has a greater effect on the torsional response than on the translational one, per Figures 8 and 9. Also, variations in the stagger angle have a much greater effect on the response amplitudes, both torsional and translational, than do the variations in the solidity. It should be noted that the design trend for modern compressors includes increased solidity and stagger angle values. Hence, these results indicate that increased forced response problems, primarily associated with increased stagger angles, might be anticipated.

Figures 10 and 11 show the effect of interblade phase angle on the coupled airfoil forced response characteristics. As seen the effect of variations in this parameter on the coupled torsional forced response are quite different than its effect on the coupled translational response. For the torsion mode, Figure 10, there is only an extreme maximum response amplitude for a 0° interblade phase angle value. For all other values considered, the response amplitude curves are relatively flat and decreased from the 0° case by approximately 75% to 85%. The coupled translational response amplitudes all exhibit an extreme maximum response amplitude, i.e. none of the amplitude response curves are relatively flat, Figure 11. Also, although an interblade phase angle value of 0° results in the maximum forced translational response amplitude, varying the interblade phase angle away from 0° results in noticably smaller decreases in this maximum amplitude than were noted for the forced torsional response. In particular, for both the torsional and the translational cases, the largest decrease in the maximum response amplitude is associated with changing the interblade phase angle value from 0° to -90°. However, the maximum forced translational response decreased only 45% whereas the corresponding forced torsional response decreased by 85%. In addition, as the smallest coupled torsional and translational response amplitudes correspond to negative interblade phase angle values, in particular -90°, then this would appear to be a possibly desirable forced response design condition. In terms of the rotor-stator interaction forced response problem, a negative interblade phase angle value corresponds to a backward traveling wave as viewed from the stator vane frame of reference and arises when the number of rotor blades is greater than the number of stator vanes.

The effect of the inlet flow Mach number on the coupled torsional and translational forced response characteristics of the representative airfoil are demonstrated in Figures 12 and 13, respectively. Increasing the Mach number, which also corresponds to decreasing the reduced frequency for a specific gust disturbance, increases both the coupled torsional and translational responses, with a very dramatic increase associated with an increase in Mach number from 0.6 to 0.8. Also, for Mach numbers of 0.6 and smaller, the increase in the maximum response amplitude is much larger for the torsional mode than for the translational mode. In addition, the forcing function frequency at which the maximum amplitude response occurs is highly dependent on the Mach number for the torsional response, but is almost independent of this forcing frequency for the translational response case.

The effect of moving the elastic axis location to the 1/4-chord and the 3/4-chord locations on the coupled forced response of the representative airfoil is presented in Figures 14 through 17. These results indicate that not only the response amplitude but also the forcing function frequency at which the maximum amplitude response occurs is strongly dependent on the position of the elastic axis. The maximum torsional and translational response amplitudes are found with the elastic axis at the 3/4-chord location. Shifting the elastic axis forward to the 1/4-chord location results in significantly decreasing both the torsional and translational response amplitudes near the airfoil torsional natural frequency but only slightly decreasing these response amplitudes near the airfoil translational natural frequency. Also, Figures 14 and 15 demonstrate that shifting the elastic axis location aft from mid-chord to 3/4-chord results in the translational response in the neighborhood of the natural torsional frequency ($\bar{\omega}/\omega_\alpha \approx 1.0$) being of the same order of magnitude as the torsional response amplitude. This is an indication of the significant additional coupling that arises when the elastic axis and the aifoil center of

gravity do not coincide. Similar results are noted when the forcing function frequency is near to the natural translational frequency, Figures 16 and 17.

To demonstrate the interaction of two very closely spaced torsional and translation modes, the bending stiffness of the representative airfoil was altered such that the ratio of the translation to torsion natural frequencies became 1.02. The variation with interblade phase angle values of these closely coupled forced torsional and translational responses was then investigated with the results presented in Figures 18 and 19. The coupled torsional response results, Figure 18, show that while this response at a frequency ratio of 0.990 decreases as the interblade phase angle is varied from 0° to $+90^\circ$, -90°, and 180°, this response increases by up to 65% at a frequency ratio of 1.015.

Figure 19 presents the variation of the forced translational response with the interblade phase angle as the parameter. In contrast to the torsional response results of Figure 18, minimal translational response is noted when the forcing function frequency is near the airfoil natural torsional frequency. However, when the forcing function frequency is near the airfoil natural translational frequency ($\bar{\omega}/\omega_\alpha \approx 1.015$), the forced translational amplitude is significant and increases as the interblade phase angle value is varied from 0° to 180°. A comparison of Figures 18 and 19 at a frequency ratio near 1.015 reveals a correspondence between the forced torsional response and the translational one. This is caused by the high degree of coupling that exists between the translation and torsional modes for this altered airfoil, even when the elastic axis coincides with the airfoil mid-chord.

Summary and Conclusions

In this investigation, the coupled structural dynamic airfoil system forced response was determined utilizing an energy balance technique. The energy input to the system per cycle of oscillation was generated by the gust and, under certain conditions, the self-induced aerodynamic forces and moments. The energy dissipation per cycle of oscillation was associated with the system structural damping, under some conditions the self-induced aerodynamic forces and moments, and the static moment term S_α. It should be noted that for the uncoupled single-degree-of-freedom case, the dissipative coupling mechanism, S_α, is not considered.

The effects of the various aerodynamic parameters on the coupled translational and torsional mode forced response of a representative airfoil was then considered. This study showed the increased coupling between the torsion and translation modes as the corresponding undamped natural frequencies approach one another. It was also demonstrated that the coupled torsional and translational forced response amplitudes of a representative airfoil increased with:

* decreased structural damping
* increased solidity values
* increased stagger angles
* increased inlet flow Mach numbers
* interblade phase angle values corresponding to forward traveling waves for the rotor-stator interaction case
* shifting of the elastic axis location aft.

It should be noted that variations in the above parameters did not affect the magnitude of the resulting forced response equally nor did they always have equivalent effects on the torsional and translational response modes. For example, increasing the stagger angle and shifting the elastic axis aft resulted in significantly larger increases in all of the response amplitudes than did increasing the solidity. Also, the interblade phase angle, for example, had a much greater effect on the coupled torsion mode responses than on the translational ones. In addition, the forcing function frequencies at which the maximum torsional and translational responses occurred did not generally correspond to the airfoil natural torsional or translational frequencies. This was because the self-induced aerodynamic forces and moments result in an aerodynamic damping effect analogous to structural damping.

Acknowledgment

Support of the research reported herein by The Air Force Office of Scientific Research, Captain Michael Francis serving as technical monitor for the project, is gratefully acknowledged.

References

1. "The Aerothermodynamics of Aircraft Gas Turbine Engines," AFAPL-TR-78-52, July 1978.

2. Fleeter, S., Jay, R. L., and Bennett, W. A., "Rotor Wake Generated Unsteady Aerodynamic Response of a Compressor Stator," ASME Journal of Engineering for Power, Vol. 100, No. 4, October 1978.

3. Fleeter, S., "Aeroelasticity Research for Turbomachine Application," AIAA Journal of Aircraft, Vol. 16, No. 5, May 1979.

4. Platzer, M. F., "Unsteady Flows in Turbomachines - A Review of Recent Developments," AGARD-CP-227, September 1977.

5. Fung, Y. C., "An Introduction to the Theory of Aeroelasticity," Dover Publications, 1969.

6. Hoyniak, D. and Fleeter, S., "Prediction of Aerodynamically Induced Vibrations in Turbomachinery Blading," ASME Symposium in Fluid/Structure Interaction in Turbomachinery, November 1981.

7. Fleeter, S., "The Fluctuating Lift and Moment Coefficients for Cascaded Airfoils in a Nonuniform Compressible Flow," AIAA Journal of Aircraft, Vol. 10, No. 2, March 1973.

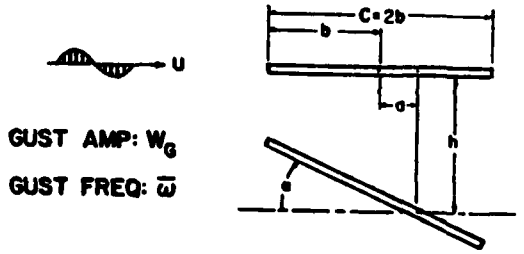

Figure 1. Airfoil and Displacement Geometry and Notation.

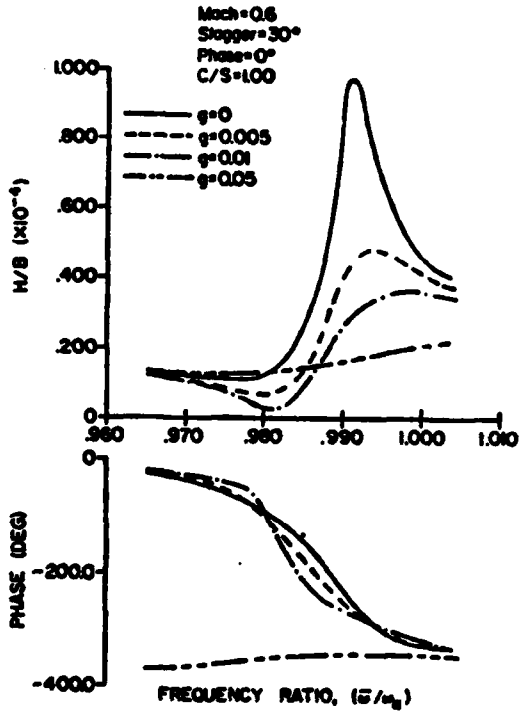

Figure 2. Structural Damping Effect on the Coupled Translational Response for ($\bar{\omega}/\omega_\alpha$) near ω_α.

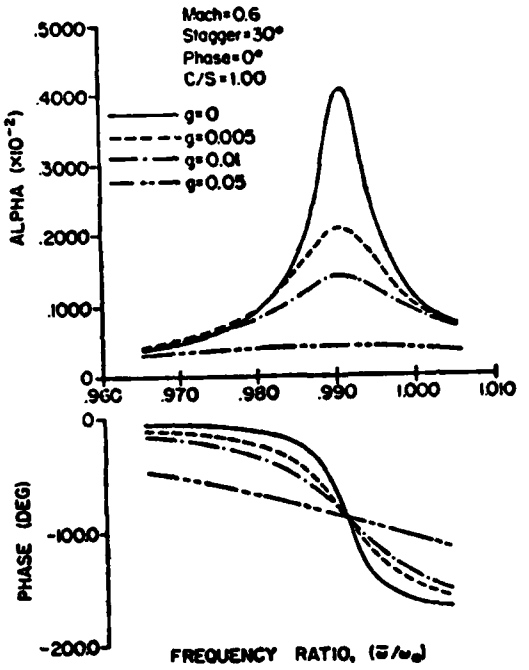

Figure 3. Structural Damping Effect on the Coupled Torsional Response Amplitude for ($\bar{\omega}/\omega_\alpha$) near ω_α.

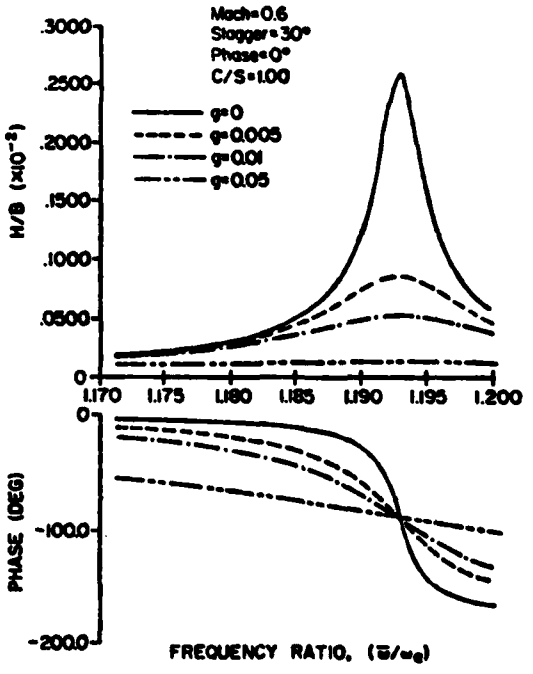

Figure 4. Structural Damping Effect on the Coupled Translational Response for ($\bar{\omega}/\omega_\alpha$) near ω_h.

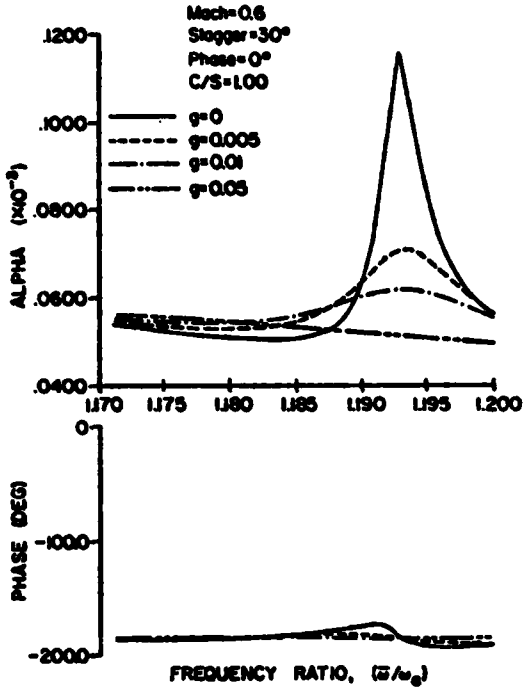

Figure 5. Structural Damping Effect on the Coupled Torsional Response for (ω/ω_α) near ω_h.

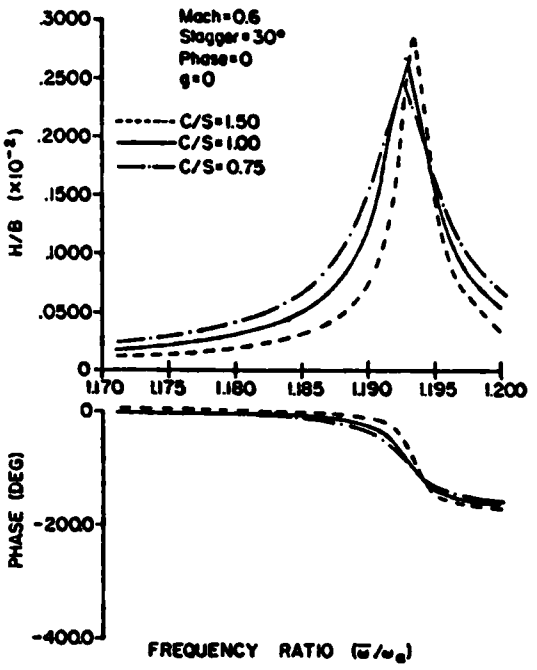

Figure 7. Cascade Solidity Effect on the Coupled Translational Response.

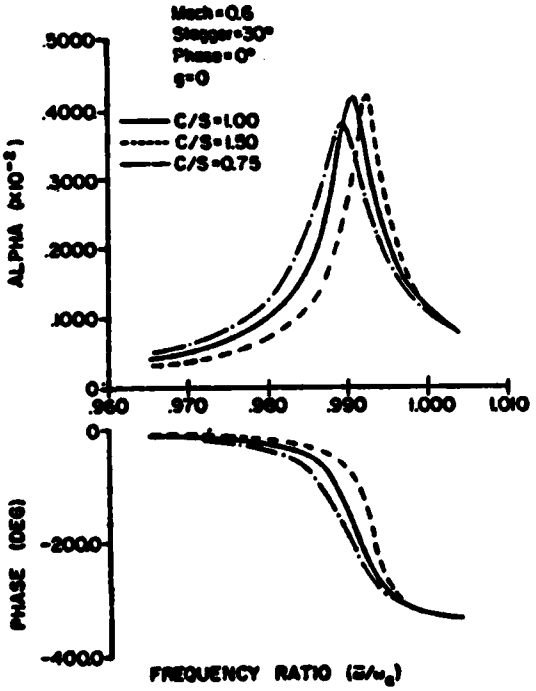

Figure 6. Cascade Solidity Effect on the Coupled Torsional Response.

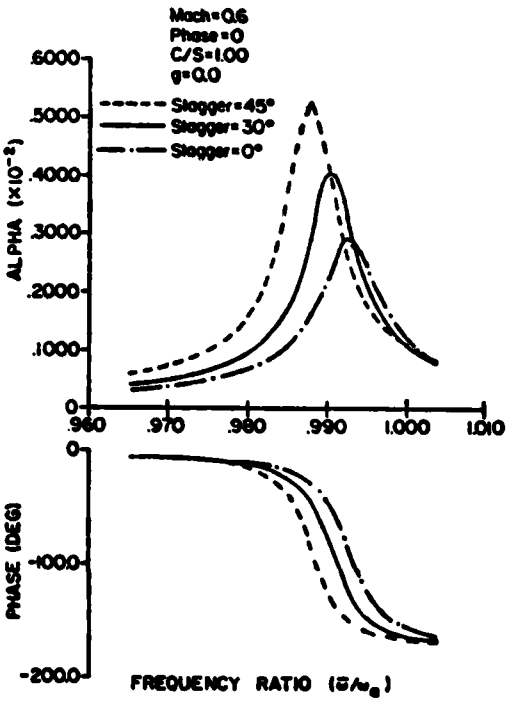

Figure 8. Effect of Stagger Angle on the Coupled Torsional Response.

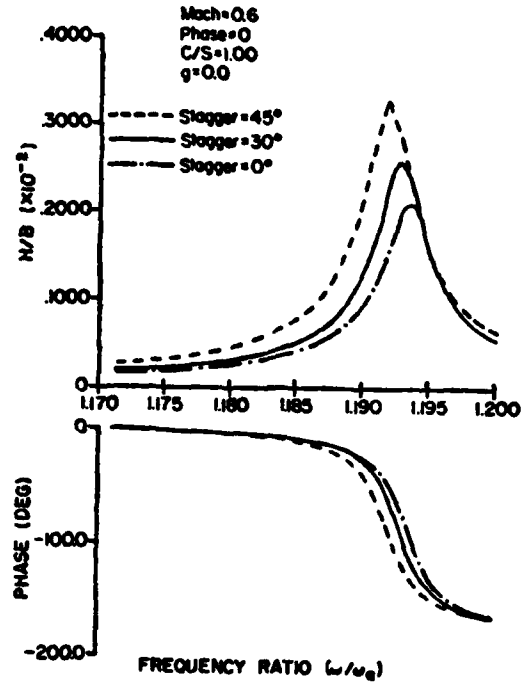

Figure 9. Effect of Stagger Angle on the Coupled Translational Response.

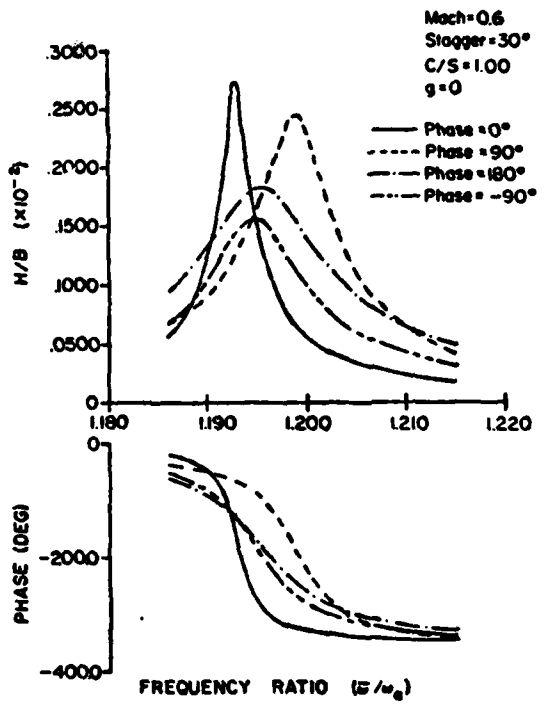

Figure 11. Effect of Interblade Phase Angle on the Coupled Translation Mode Response.

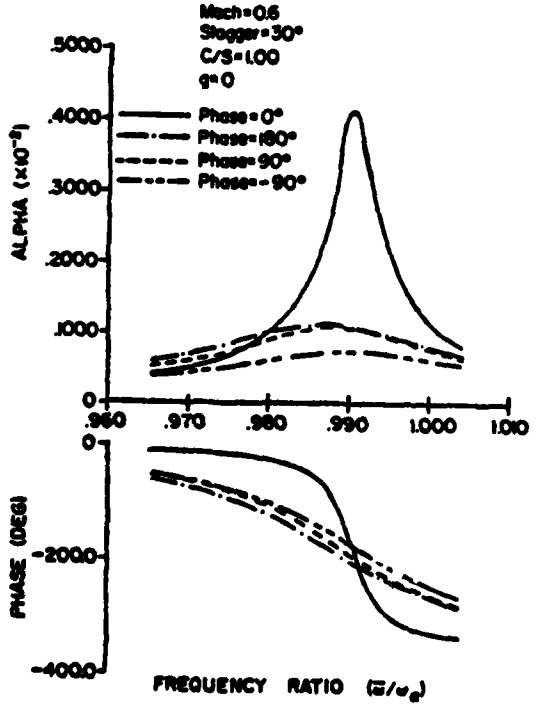

Figure 10. Effect of Interblade Phase Angle on the Coupled Torsion Mode Response.

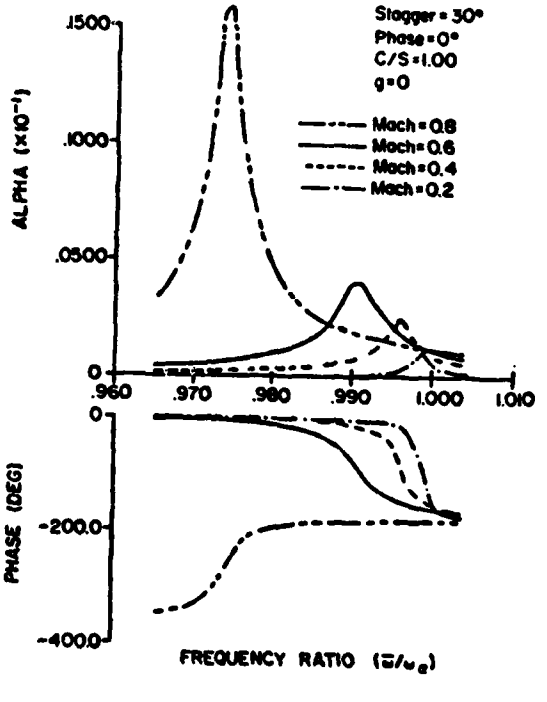

Figure 12. Inlet Mach Number Effect on the Coupled Torsional Response.

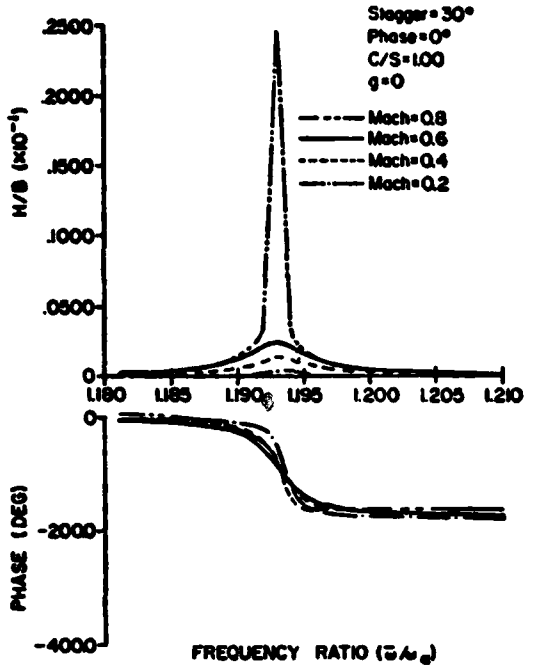

Figure 13. Inlet Mach Number Effect on the Coupled Translational Response.

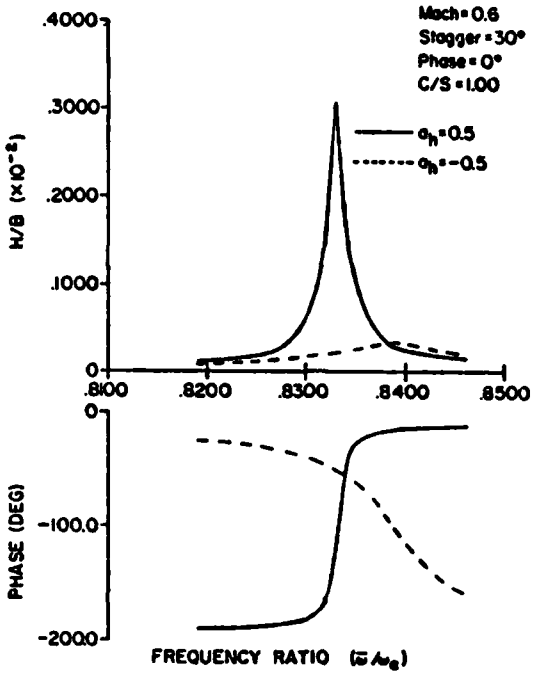

Figure 15. Effect of Elastic Axis Location on the Coupled Translational Response for $(\bar{\omega}/\omega_\alpha)$ near ω_α.

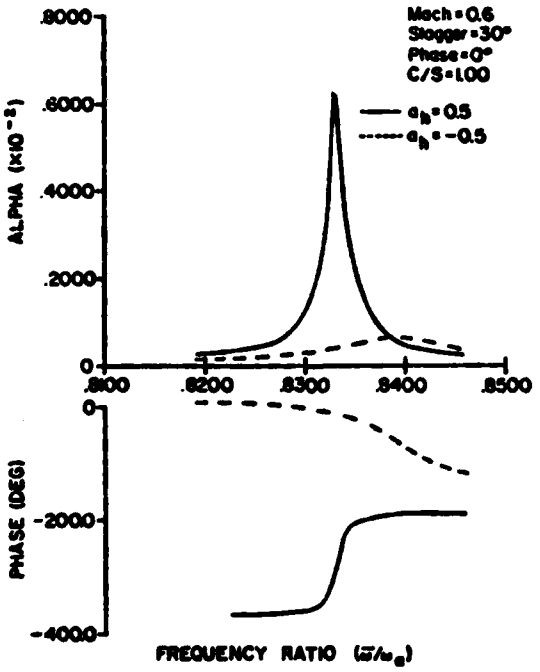

Figure 14. Effect of Elastic Axis Location on the Coupled Torsional Response for $(\bar{\omega}/\omega_\alpha)$ near ω_α.

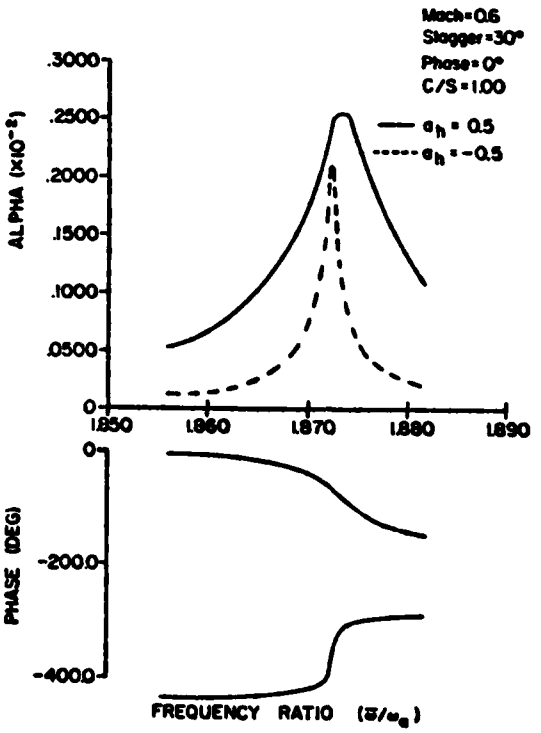

Figure 16. Effect of Elastic Axis Location on the Coupled Torsional Response for $(\bar{\omega}/\omega_\alpha)$ near ω_h.

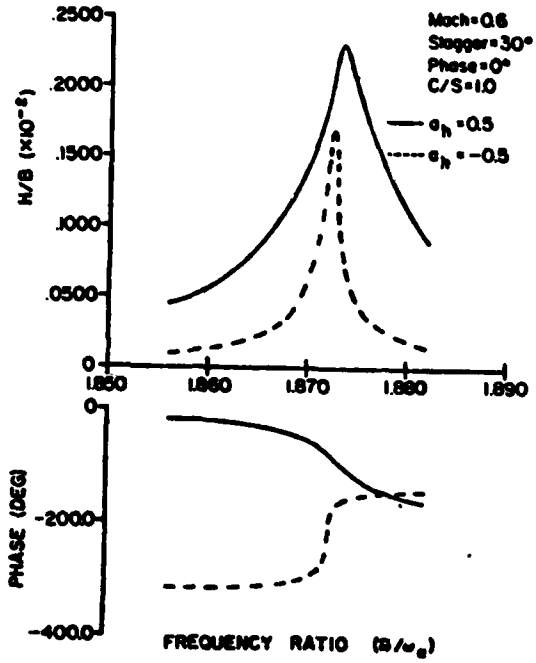

Figure 17. Effect of Elastic Axis Location on the Coupled Translational Response for $(\bar{\omega}/\omega_\alpha)$ near ω_h.

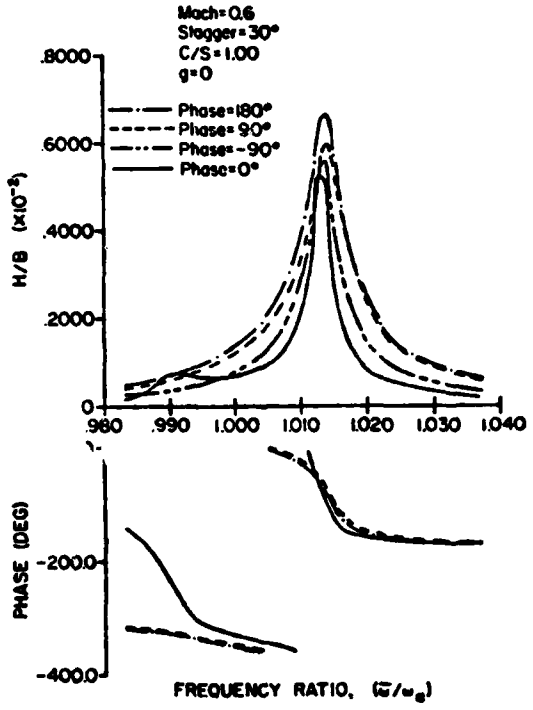

Figure 19. Interblade Phase Angle Effect on the Coupled Translational Response for Nearly Equal Natural Frequencies.

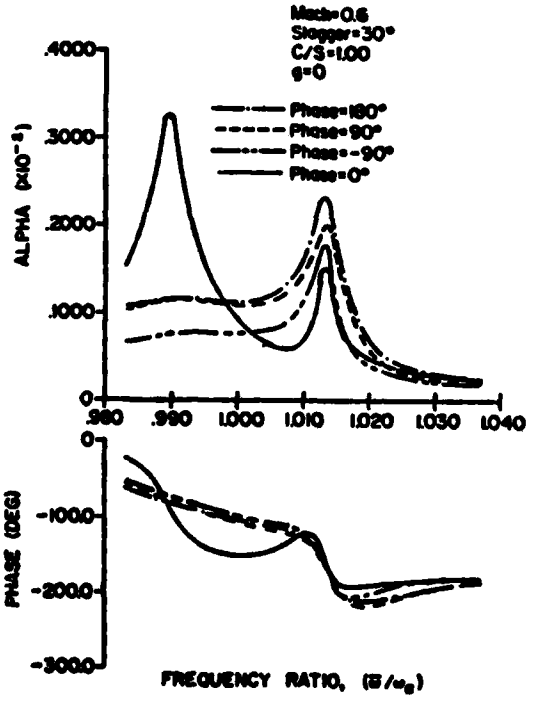

Figure 18. Interblade Phase Angle Effect on the Coupled Torsional Response for Nearly Equal Natural Frequencies.

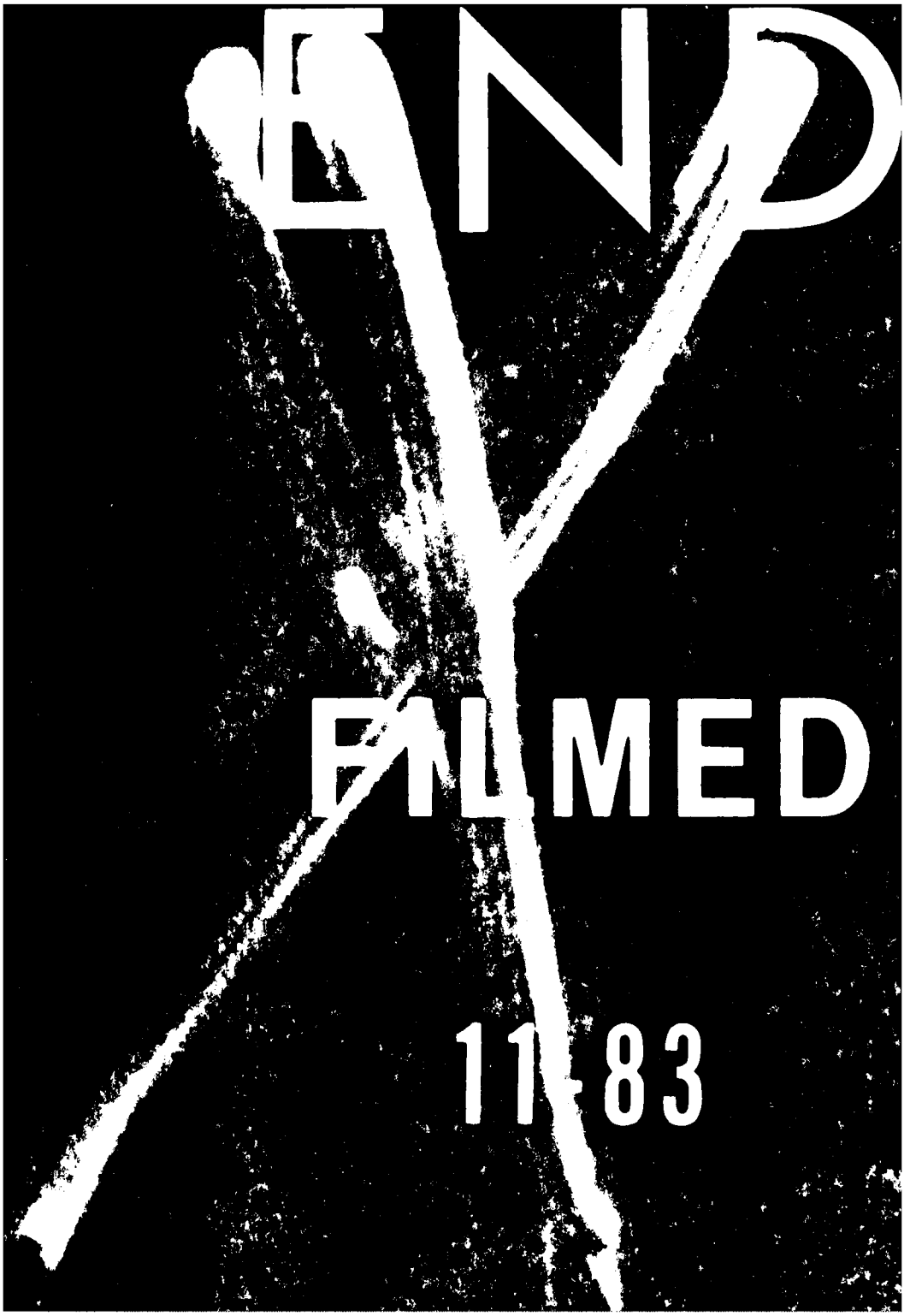
END
FILMED
11-83

AD A133 853 RESEARCH ON AERO-THERMODYNAMIC DISTORTION INDUCED STRUCTURAL DYNAMIC RESP..(U) PURDUE UNIV LAFAYETTE IN SCHOOL OF MECHANICAL ENGINEERING S FLEETER JUN 83

UNCLASSIFIED ME-TSPC-TR-83-04 AFOSR-TR-83-0737 F/G 21/5 NL

2/2

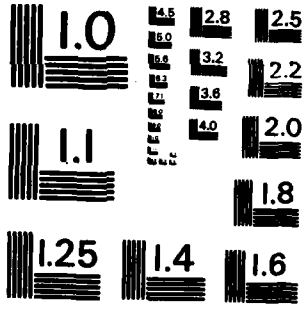

MICROCOPY RESOLUTION TEST CHART
NATIONAL BUREAU OF STANDARDS - 1963 - A

SUPPLEMENTARY

INFORMATION

AD-A133 853

UNCLASSIFIED changed to final
SECURITY CLASSIFICATION OF PAGE (When Data Entered)

REPORT DOCUMENTATION PAGE		READ INSTRUCTIONS BEFORE COMPLETING FORM
1. REPORT NUMBER: AFOSR-TR-83-0737	2. GOVT ACCESSION NO.	3. RECIPIENT'S CATALOG NUMBER
4. TITLE (and Subtitle): RESEARCH ON AERO-THERMODYNAMIC DISTORTION INDUCED STRUCTURAL DYNAMIC RESPONSE OF MULTI-STAGE COMPRESSOR BLADING		5. TYPE OF REPORT & PERIOD COVERED: ~~Annual~~ FINAL 15 Apr 82 - 14 Apr 83
		6. PERFORMING ORG. REPORT NUMBER
7. AUTHOR(s): SANFORD FLEETER		8. CONTRACT OR GRANT NUMBER(s): AFOSR-82-0188
9. PERFORMING ORGANIZATION NAME AND ADDRESS: PURDUE UNIVERSITY, DEPT OF MECHANICAL ENGINEERING, WEST LAFAYETTE, IN 47907		10. PROGRAM ELEMENT PROJECT, TASK AREA & WORK UNIT NUMBERS: 61102F, 2307/A4
11. CONTROLLING OFFICE NAME AND ADDRESS: AIR FORCE OFFICE OF SCIENTIFIC RESEARCH/NA, BOLLING AFB, DC 20332		12. REPORT DATE: June 1983
		13. NUMBER OF PAGES: 49
14. MONITORING AGENCY NAME & ADDRESS(if different from Controlling Office)		15. SECURITY CLASS. (of this report): Unclassified
		15a. DECLASSIFICATION DOWNGRADING SCHEDULE

16. DISTRIBUTION STATEMENT (of this Report)

Approved for Public Release; Distribution Unlimited.

17. DISTRIBUTION STATEMENT (of the abstract entered in Block 20, if different from Report)

18. SUPPLEMENTARY NOTES

19. KEY WORDS (Continue on reverse side if necessary and identify by block number)

TURBOMACHINERY
COMPRESSORS
FORCED VIBRATION
FLUID MECHANICS
AERO-THERMODYNAMIC DISTORTION
UNSTEADY FLOW
INLET FLOW

20. ABSTRACT (Continue on reverse side if necessary and identify by block number)

The structural dyanmic response of turbomachinery components to aero-thermodynamic distortion induced excitations is an item of major concern in the design of advanced gas turbine engines. The rotor speeds at which these resonant forced responses occur can be predicted with Campbell diagrams. However, due to the inadequacies of the existing time-variant aerodynamic models, no accurate prediction can currently be made for the amplitude of the resulting stresses. The overall objective of this research program is to quantitatively investigate the fundamental phenomena relevant to

DD FORM 1 JAN 73 1473 EDITION OF 1 NOV 65 IS OBSOLETE

UNCLASSIFIED
SECURITY CLASSIFICATION OF THIS PAGE (When Data Entered)

acrothermodynamic distortion induced structural dynamic blade response in multi-stage gas turbine fans and compressors. Unique unsteady aerodynamic data will be obtained to validate and indicate necessary refinements to state-of-the-art analyses and to direct the modeling of new analyses. Also, for the first time, a first principles capability to predict the vibrational response amplitude of blading due to aerodynamic excitations will be developed. This report summarizes the progress and results obtained during the first year of this program. These include: the dynamic instrumentation of the first-state vane row of a three-stage research compressor; the design, specification and initiation of the developmemt of the dynamic data acquisition and analysis system; the initiation of the development of the necessary data analysis and calibration techniques; and the theoretical development of a unique coupled mode structural dynamic blade response analysis based on an energy balance technique.

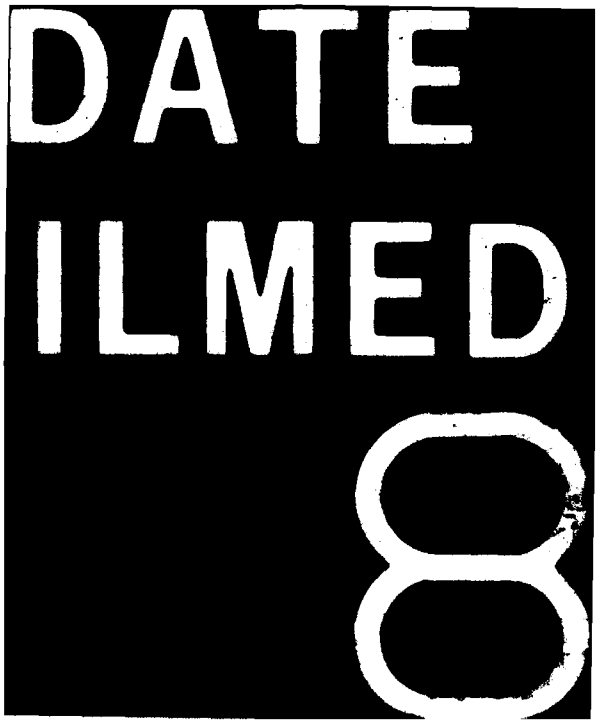
DATE
ILMED
8